Materials and Structures (2024) 57:206
https://doi.org/10.1617/s11527-024-02465-0

RILEM TC 281-CCC - CARBONATION OF CONCRETE WITH SUPPLEMENTARY CEMENTITIOUS MATERIALS

Report of RILEM TC 281-CCC: insights into factors affecting the carbonation rate of concrete with SCMs revealed from data mining and machine learning approaches

A. Vollpracht · G. J. G. Gluth · B. Rogiers · I. D. Uwanuakwa · Q. T. Phung · Y. Villagran Zaccardi · C. Thiel · H. Vanoutrive · J. M. Etcheverry · E. Gruyaert · S. Kamali-Bernard · A. Kanellopoulos · Z. Zhao · I. M. Martins · S. Rathnarajan · N. De Belie

Received: 26 March 2024 / Accepted: 8 September 2024

Abstract The RILEM TC 281–CCC ‘‘Carbonation of concrete with supplementary cementitious materials’’ conducted a study on the effects of supplementary cementitious materials (SCMs) on the carbonation rate of blended cement concretes and mortars. In this context, a comprehensive database has been established, consisting of 1044 concrete and mortar mixes with their associated carbonation depth data over time. The dataset comprises mix designs with a large variety of binders with up to 94% SCMs, collected from the literature as well as unpublished testing reports. The data includes chemical composition and physical properties of the raw materials, mix-designs, compressive strengths, curing and carbonation testing conditions. Natural carbonation was recorded for several years in many cases with both indoor and outdoor results. The database has been analysed to investigate the effects of binder composition and mix design, curing and preconditioning, and relative humidity on the carbonation rate. Furthermore, the accuracy of accelerated carbonation testing as well as possible correlations between compressive strength and carbonation resistance were evaluated. One approach to summerise the physical

Supplementary Information The online version contains supplementary material available at https://doi.org/10.1617/s11527-024-02465-0.

This article was prepared within the framework of RILEM TC 281-CCC. The article has been reviewed and approved by all members of the TC.

TC 281-CCC Membership
TC Chair: Prof. Nele De Belie.
Deputy Chair: Prof. Susan Bernal Lopez.

Members: Natalia Alderete, Carmen Andrade, Ueli Angst, Tushar Bansal, Véronique Baroghrl-Bouny, Muhammed P.a. Basheer, Nele De Belie, Susan Bernal Lopez, Hans D. Beushausen, Leon Black, Aires Camoes, Servando Chinchon-Paya, Özlem Cizer, Gisela Paola Cordoba, Martin Cyr, Patrick Dangla, Yuvaraj Dhandapani, Katja Dombrowski-Daube, Vilma Ducman, Yogarajah Elakneswaran, Jan Elsen, Juan Manuel Etcheverry, Miren Etxeberria, Ana Maria Fernandez-Jimenez, Lander Frederickx, Cassandre L Galliard, Inès Garcia Loderieo, Daniel Geddes, Christoph Gemlen, Mette Geiker, Guoqing Geng, Bahman Ghiassi, Gregor Gluth, Cyrill Grengg, Elke Gruyaert, R. Doug Hooton, Bruno Huet, Yu Huang, Andres Idiart, Ivan Ignjatovic, Kei-Ichi Imamoto, Shiju Joseph, Zuquan Jin, Siham Kamali-Bernard, Antonis Kanellopoulos, Xinyuan Ke, Sylvia Kessler, Heejeong Kim, Sabine Kruschwitz, Namkon Lee, Bin Li, Juan Li, Ning Li, Tung Chai Ling, Zhiyuan Liu, Qing-feng Liu, Barbara Lothenbach, Jingzhou Lu, Isabel Martins, José Fernando Martirena-Hernandez, César Medina Martinez, Renjie Mi, Fabrizio Moro, Shishir Mundra, Yeakleang Muy, Marija Nedeljkovic, Kolawole A. Olonade, José Pacheco, Christian Paglia, Angel Palomo, Sol Moi Park, Ravi Patel, Janez Perko, Quoc Tri Phung, Elodie Piolet, John L. Provis, Francisca Puertas, Sundar Rathnarajan, Nuria Rebolledo, Bart Rogiers, Marlene Sakoparnig, Javier Sanchez Montero, Francesco Santoto, Sriram Pradeep Saridhe, Karen Scrivener, Marijana Serdar, Xinyu Shi, Zhenguo Shi, Kosmas K. Sideris, Ruben Snellings,

Published online: 23 October 2024

and chemical resistance in one parameter is the ratio of water content to content of carbonatable CaO ($w/CaO_{reactive}$ ratio). The analysis revealed that the $w/CaO_{reactive}$ ratio is a decisive factor for carbonation resistance, while curing and exposure conditions also influence carbonation. Under natural exposure conditions, the carbonation data exhibit significant variations. Nevertheless, probabilistic inference suggests that both accelerated and natural carbonation processes follow a square-root-of-time behavior, though accelerated and natural carbonation cannot be converted into each other without corrections. Additionally, a machine learning technique was employed to assess the influence of parameters governing the carbonation progress in concretes.

Keywords Natural carbonation · Accelerated carbonation · SCMs · Database

1 Introduction

In order to study the effects of concrete composition, curing, pre-storage and exposure conditions on carbonation kinetics the RILEM TC 281-CCC ''Carbonation of concrete with supplementary cementitious materials'' has set up a database with results of carbonation experiments. The data were collected from literature as well as unpublished research and material testing reports [1–54]. Throughout the whole database, the phenolphthalein test was used to measure the carbonation depth at different exposure times.

The database includes 1044 concrete and mortar mixes, manufactured with single cements or with binary and ternary combinations of SCM with cements. The types of cements and SCM used are listed in Table 1. The water/binder ratio of the

Matteo Stefanoni, Charlotte Thiel, Karl Christian Thienel, Ilda Tole, Ikenna D. Uwanuakwa, Luca Valentini, Philip Van Den Heede, Hanne Vanoutrive, Yury Andrés Villagran Zaccardi, Visalakshi Talakokula, Anya Vollpracht, Stefanie Von Greve-Dierfeld, Brant Walkley, Fazhou Wang, Ling Wang, Zhendi Wang, Jinxin Wei, Lia Weiler, Bei Wu, Chuansheng Xiong, Yan Yao, Guang Ye, Maciej Zajac, Cheng Zhang, Zengfeng Zhao, Semion Zhutovsky.

A. Vollpracht (✉)
Institute of Building Materials Research, RWTH Aachen University, Aachen, Germany
e-mail: vollpracht@ibac.rwth-aachen.de

G. J. G. Gluth
Division 7.4 Technology of Construction Materials, Bundesanstalt für Materialforschung und -prüfung (BAM), Berlin, Germany

B. Rogiers · Q. T. Phung
Sustainable Waste & Decommissioning, Belgian Nuclear Research Centre (SCK CEN), Mol, Belgium

I. D. Uwanuakwa
Department of Civil Engineering, Near East University, Mersin 10, Turkey

Y. Villagran Zaccardi
Materials and Chemistry Unit, Flemish Institute for Technological Research (VITO), Mol, Belgium

C. Thiel
Construction Materials, Department of Civil Engineering, OTH Regensburg, Regensburg, Germany

H. Vanoutrive · E. Gruyaert
Materials and Constructions, Department of Civil Engineering, KU Leuven, Ghent, Belgium

J. M. Etcheverry · N. De Belie
Department of Structural Engineering and Building Materials, Magnel-Vandepitte Laboratory, Ghent University, Ghent, Belgium

S. Kamali-Bernard
Département de Génie Civil e Urbain, Institut National des Sciences Appliquées (INSA-Rennes), Université de Rennes, Rennes, France

A. Kanellopoulos
School of Physics, Engineering & Computer Science, Centre for Engineering Research, University of Hertfordshire, Hertfordshire, UK

Z. Zhao
Department of Structural Engineering, College of Civil Engineering, Tongji University, Shanghai, China

I. M. Martins
Departamento de Materiais, Laboratório Nacional de Engenharia Civil, Lisbon, Portugal

S. Rathnarajan
Department of Civil Engineering, Indian Institute of Technology Madras, Chennai, India

Table 1 Overview of the cements and supplementary cementitious materials (SCMs) of the concretes and mortars in the database, including the abbreviations used throughout this document

Cements*		SCMs	
Type	Number	Type	Number
CEM I	97	siliceous fly ash (sFA)	66
CEM II/A-D	1	calcareous fly ash (cFA)	2
CEM II/A-L or LL	14	siliceous bottom ash (sBA)	1
CEM II/A-M (S-LL)	1	ground granulated blast-furnace slag (GGBS)	31
CEM II/A-S	2	calcined clay (CC) (incl. metakaolin (MK))	19
CEM II/A-V	4	limestone (L)	3
CEM II/B-L or LL	11	natural pozzolan (nP)	3
CEM II/B-M (S-L or LL)	23	silica fume (SF)	4
CEM II/B-M (T-LL)	1	steel slag (SWS)	1
CEM II/B-M (V-LL)	3		
CEM II/B-P	4		
CEM II/B-S	18		
CEM II/B-V	22		
CEM III/A	64		
CEM III/B	38		
CEM III/C	2		
CEM IV/A	1		
CEM IV/B	1		
CEM V/A	1		

*Notation of EN 197: CEM I: Portland cement, CEM II: Portland composite cement (A: clinker content 80–94 wt.% (exception: CEM II/A-D contains 90–94 wt.% clinker), B: clinker content 65–79 wt.%), CEM III: blast-furnace slag cement (A: clinker content 35–64 wt.%, B: clinker content 20–34 wt.%, C: clinker content 5–19 wt.%), CEM IV: pozzolan cement (A: clinker content 65–89 wt.%, B: clinker content 45–64 wt.%), CEM V: composite cement (A: clinker content 40–64 wt.%), D: silica fume, L and LL: limestone (with different TOC limits), S: GGBS, V: siliceous fly ash, T: burnt oil shale, P: natural pozzolan

concretes and mortars varies between 0.26 and 0.75. In many cases, several concretes were prepared with the same cement and/or SCM, but with different w/b ratios or replacement levels. The database, which is provided as an electronic supplement, contains detailed information on the individual mix designs.

Since a high amount of data is available for binary or ternary mixes with siliceous fly ashes and GGBSs, Sects. 3 to 7 focus on those mixes and compare their carbonation kinetics with those of plain Portland cement mixes. In the first step the carbonation rate is fitted (Sect. 2), and then, in Sects. 3 to 7, some of the influencing factors pointed out in the literature review of TC 281-CCC [55] are further investigated using the collected data. Finally, in Sect. 8, the entire dataset is modelled collectively, using probabilistic inference, attempting to account for the different influencing factors in a mechanistic way, and using machine learning, to explore how far we can go in predicting carbonation depth given the available data.

2 Determination of carbonation rate

Different approaches have been used in literature to determine the carbonation rate of concrete and mortar under natural conditions. Most authors determine a best-fit line of carbonation depths d_c versus square root of time ($\sqrt{t}$). However, in some references, also single measurements at an instantaneous time are used, and the rate is calculated by assuming that the carbonation depth is zero at the beginning of the test (e. g. [16, 21]). In [21], a testing age of 140 d is suggested. As another option, 365 d were considered in this evaluation.

In this section, different methods to determine the carbonation depth are compared with regard to their

reliability in predicting long-term carbonation. The following approaches are used:

1) Based on the measured carbonation depths d_c within the first year, the carbonation rate k_c is calculated as the slope of a best fit line of d_c vs. $\sqrt{t}$ as shown in Fig. 1a. Often the calculated initial carbonation depth is not zero (see Fig. 1b, full black line). A positive intercept is accepted, and the carbonation rate is taken as calculated (e.g., 0.37 mm/$\sqrt{}$d for the mix plotted with green triangles). Since a negative intercept is not possible from a physical point of view, the intercept is fixed at zero in these cases (dotted black line in Fig. 1b). For the prediction of long-term carbonation usually only the carbonation rate is considered. This means that the intercept is neglected in the long-term and the carbonation depth at later ages is calculated as:

$$d_{c,p}(t) = k_c \cdot \sqrt{t} \quad (1)$$

$d_{c,p}$ predicted carbonation depth at age t in mm, t duration of carbonation exposure in d, k_c carbonation rate in mm/$\sqrt{}$t

2) The original best fit line from the first year's measurements including the intercept b is used to predict later age carbonation depth:

$$d_{c,p} = k_c \cdot \sqrt{t} + b \quad (2)$$

Results for positive and negative intercepts are plotted separately.

3) Carbonation rates are calculated from single measurements after alternatively 365 ± 10 d (approach 3a) or 140 ± 10 d (approach 3b) and carbonation depths at later ages are predicted according to Eq. (1)

Fig. 2 Time-dependent statistical evaluation of the accuracy of different methods to determine the carbonation rate (Boxes: 25–75% range, squares: average, horizontal lines: median, whiskers: twofold standard deviation, diamonds: potential outliers, n: number of measurements)

The database contains long-term results up to an age of 6559 d (18 a). In order to determine the accuracy of the estimation in the course of time, all datasets with at least two years duration were collected and the results were grouped according to testing age. The carbonation depths at the respective measuring times were estimated according to the approaches 1) to 3) as described above. The error is then calculated according to Eq. (3).

$$e = d_{c,p} - d_{c,m} \quad (3)$$

where $d_{c,m}$ is the measured carbonation depth in mm.

Figure 2 shows the statistical evaluation of the errors in carbonation depths for different carbonation times (regardless of the mixture composition). In this graph, only indoor data (room climate) for natural carbonation were considered. The number of data points is quite different for the different testing times and in some cases, it can be questioned whether the data are representative, because of the limited amount of results. Despite this problem some trends are visible: All three approaches used in this study tend to overestimate carbonation depths at later ages. As expected, the errors increase with time, as the rate is calculated with an error and the rate gets magnified by the multiplication with $\sqrt{t}$. The highest errors can be found for the prediction based on a single measurement after about 140 d (approach 3b), from

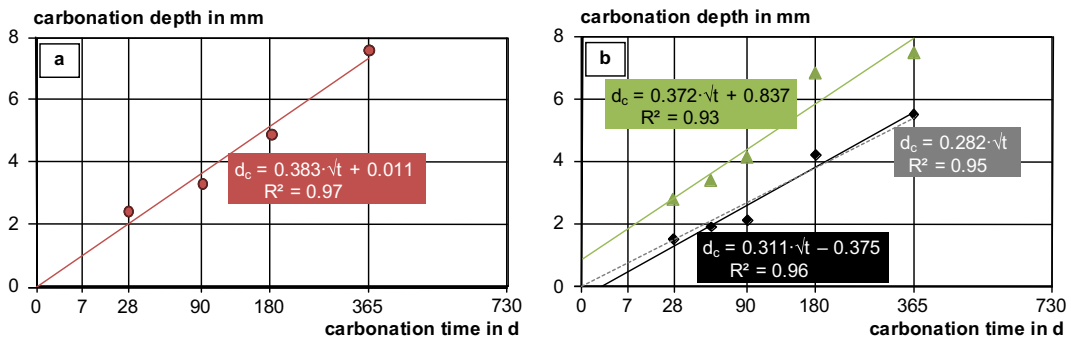

Fig. 1 Determination of carbonation rate: (**a**) ideal example of best fit; (**b**) best fit with intercept [56]

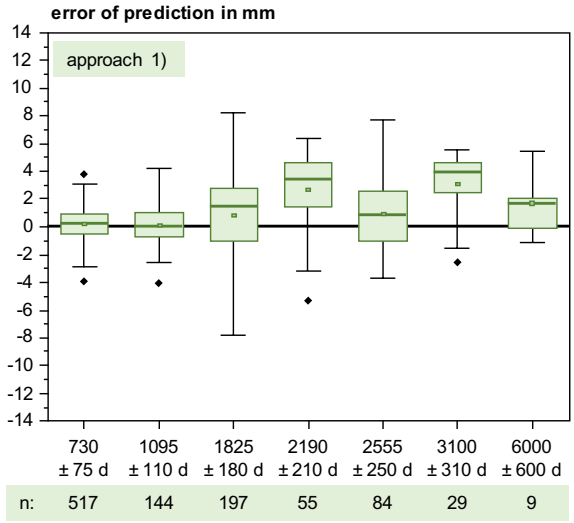
error of prediction in mm
approach 1)
14
12
10
8
6
4
2
0
-2
-4
-6
-8
-10
-12
-14
730 ± 75 d
1095 ± 110 d
1825 ± 180 d
2190 ± 210 d
2555 ± 250 d
3100 ± 310 d
6000 ± 600 d
n: 517 144 197 55 84 29 9

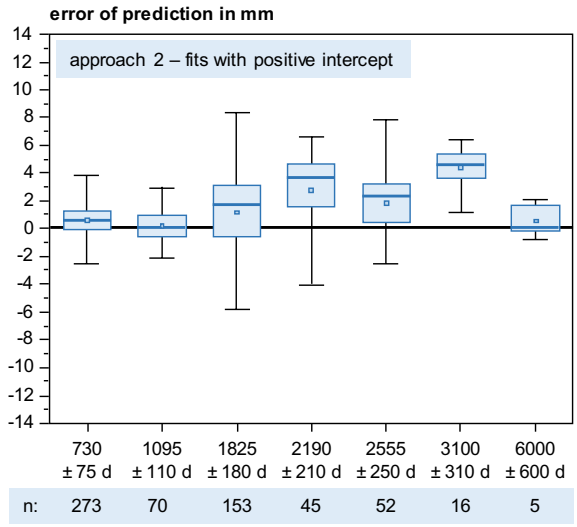
error of prediction in mm
approach 2 – fits with positive intercept
14
12
10
8
6
4
2
0
-2
-4
-6
-8
-10
-12
-14
730 ± 75 d
1095 ± 110 d
1825 ± 180 d
2190 ± 210 d
2555 ± 250 d
3100 ± 310 d
6000 ± 600 d
n: 273 70 153 45 52 16 5

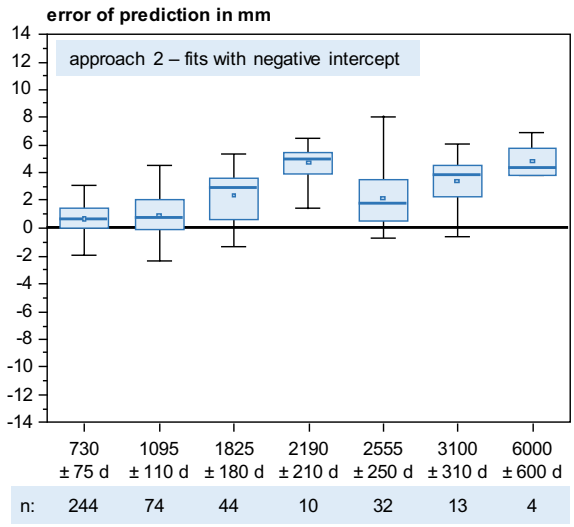
error of prediction in mm
approach 2 – fits with negative intercept
14
12
10
8
6
4
2
0
-2
-4
-6
-8
-10
-12
-14
730 ± 75 d
1095 ± 110 d
1825 ± 180 d
2190 ± 210 d
2555 ± 250 d
3100 ± 310 d
6000 ± 600 d
n: 244 74 44 10 32 13 4

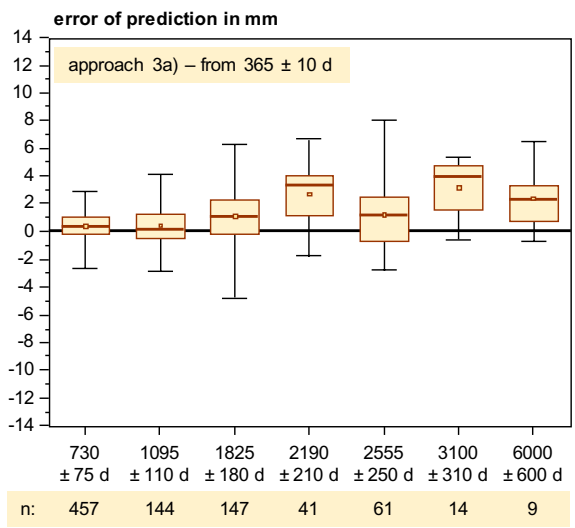
error of prediction in mm
approach 3a) – from 365 ± 10 d
14
12
10
8
6
4
2
0
-2
-4
-6
-8
-10
-12
-14
730 ± 75 d
1095 ± 110 d
1825 ± 180 d
2190 ± 210 d
2555 ± 250 d
3100 ± 310 d
6000 ± 600 d
n: 457 144 147 41 61 14 9

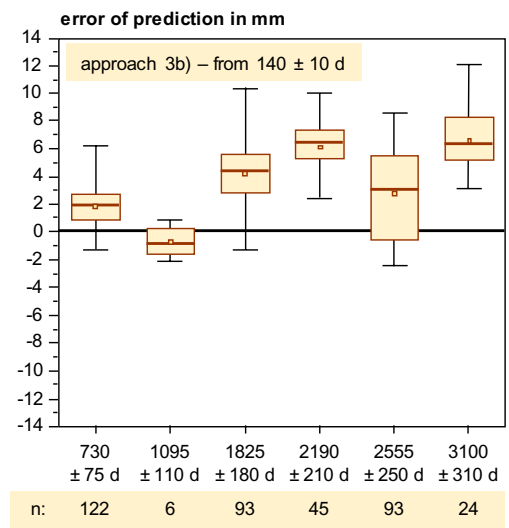
error of prediction in mm
approach 3b) – from 140 ± 10 d
14
12
10
8
6
4
2
0
-2
-4
-6
-8
-10
-12
-14
730 ± 75 d
1095 ± 110 d
1825 ± 180 d
2190 ± 210 d
2555 ± 250 d
3100 ± 310 d
n: 122 6 93 45 93 24

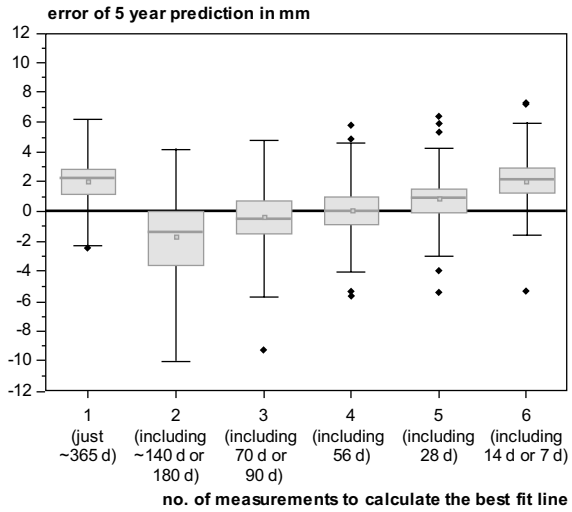

Fig. 3 Influence of the number of measuring times on the error of the prediction after five years of carbonation (Boxes: 25–75% range, squares: average, horizontal lines: median, whiskers: twofold standard deviation, diamonds: potential outliers, n = 113)

which it can be concluded that this testing period is too short and not preferable for estimating later-age carbonation depths. Approach 2 also results in quite high errors, if the intercept is negative (right figure). Hence it is reasonable to correct the fit to $b = 0$ mm in these cases, as it was carried out in approach 1.

The first approach gives the smallest errors and will be used for further analysis. It should be noted that even with this method, the error variation is significant. The prediction based on one year's results is on average quite good, but for specific datasets, the discrepancies can be quite high (errors of prediction up to ± 8 mm are observed after 5 years of exposure).

The specific testing regimes differ considerably within the database. In some cases, only very few measurements were performed, in other references up to 10 carbonation times were tested within the first year. To determine how many measurement times are appropriate to predict the carbonation rate in a reliable way, the available data until about 5 years (1825 ± 180 d) of exposure were chosen as an exemplary data set. From this data-set, only the tests with at least 6 measurement times within the first year were selected ($n = 113$). For each of these tests, the best fit line was calculated using 1 to 6 measurement times, starting at about one year and gradually including earlier test ages. The error of the prediction was calculated as described above and the results are shown in Fig. 3.

The best approximation of the measured values is found for four testing times between 56 and 365 d. Including data for shorter carbonation times does not lead to a better prognosis, but rather seems to be counterproductive. A reason for this could be the higher inaccuracy of the measurement at low carbonation depths. Nevertheless, all measurements were considered to be consistent with and comparable to previous studies.

For accelerated carbonation, the testing times are shorter; nevertheless, the carbonation rate was determined in the same way, i.e., according to approach 1. Some authors only tested one point in time. In these cases, the intercept was assumed to be zero. The calculated carbonation rates are included in the electronic supplement.

3 Natural carbonation

3.1 Effect of w/$CaO_{reactive}$ on carbonation in indoor climate

Leemann et al. established a correlation between the ratio $w/CaO_{reactive}$ and the carbonation rate of blended cement mortars and concretes [31, 32]. In this ratio, w is the mass of water in the mix, and $CaO_{reactive}$ is the mass of CaO in the binder that is able to react with the water to form hydration products. The effect of w on the carbonation rate derives from the fact that the water/binder ratio determines the porosity and thereby the diffusion coefficient of CO_2 in cementitious materials. The inverse relationship between $CaO_{reactive}$ and carbonation rate can be understood by considering that a higher volume fraction of hydration products in a material causes a higher CO_2 binding capacity of the material and, thus, a slower progress of the carbonation front. In their first study [31], Leemann and co-workers calculated $CaO_{reactive}$ by subtracting the CaO in the limestone powder ($CaCO_3$) of the employed cements from the total CaO in the binder, while no correction was made for CaO in unreactive phases that might be present in the fly ash in a CEM II/B-M (V-LL) and the GGBS in a CEM III/B. In their subsequent work [32], in which several GGBS-containing cements and two fly ash-containing cement were studied, the same approach was

followed, *i.e.*, only the CaO in limestone was subtracted from the total CaO to obtain $CaO_{reactive}$.

For the present evaluation, the reactive CaO was calculated according to Eq. (4),

$$CaO_{reactive} = CaO_{total} - CaO_{CaCO3\ init} - CaO_{CaSO4} \quad (4)$$

where CaO_{total} is the total amount of CaO in the binder, $CaO_{CaCO3\ init}$ is the CaO in the limestone powder ($CaCO_3$) of the binder, and CaO_{CaSO4} is the CaO in the sulfate carrier (gypsum, hemihydrate, anhydrite) of the binder.

Equation (4) assumes that CaO contained in limestone as well as CaO contained in the sulfate carrier of the cements do not participate in CO_2 binding in the hydrated cements. CaO in the limestone of the cements can be assumed to react to form monocarboaluminate and/or hemicarboaluminate (and to remain partly unreacted at high substitution rates) during hydration [57, 58]. On carbonation, monocarboaluminate and hemicarboaluminate eventually yield calcite [59] and thus do not contribute to additional binding of atmospheric CO_2. The sulfate carrier is mainly consumed by formation of ettringite and/or monosulfoaluminate during cement hydration [60]; when monosulfoaluminate is carbonated, more ettringite is formed [59]. At advanced stages of carbonation, the ettringite decomposes, with the released sulfate anions eventually precipitating as calcium sulfate (gypsum or hemihydrate) [59, 61]. Thus, the above assumption that CaO in limestone and the sulfate carrier does not contribute to CO_2 binding, and thus is not included in the calculation of $CaO_{reactive}$, is justified.

An additional assumption, implicitly contained in Eq. (4), is that all CaO contained in the SCMs (*i.e.*, not in limestone or the sulfate carrier) in the cements is available to form hydration products. This assumption may not be fully accurate, as inert Ca-bearing phases can be present in SCMs. For example, GGBS may contain merwinite and/or gehlenite, and fly ashes may contain anorthite. However, the fraction of inert Ca-phases in GGBS and siliceous fly ashes is generally low, while virtually all of the CaO in these materials is in their reactive glassy phase [60]; thus, the error introduced by not excluding the CaO in inert phases from $CaO_{reactive}$ is likely very minor for most GGBS- and hard coal fly ash-blended cements. For cements with other SCMs, such as calcined clays, natural pozzolans or lignite fly ashes, which may contain considerable amounts of inert Ca-bearing phases such as feldspars, augite or gehlenite, respectively, the error may be more significant in some cases, *i.e.*, the ratio $w/CaO_{reactive}$, calculated with Eq. (4), may be significantly lower than the value that would be obtained with a more accurate estimate of $CaO_{reactive}$. The calculation of the latter value would require knowledge of the abundances of the inert phases in all SCMs of a cement; however, in the majority of published studies, these were not reported.

Figure 4 shows the results for the different binder types tested under laboratory conditions at 20 °C and 60–65% RH. For most binders the carbonation rates after 2 d of curing are higher than the average line for 7 d curing, indicating that the hydration degree at the beginning of the carbonation test was too low and negatively impacted the carbonation resistance. Most results for 3 and 4 d of curing fall in the range of the 7 d curing results. All binder types show the expected trend towards increasing carbonation rates with increasing $w/CaO_{reactive}$, though the scatter of the data is quite high. Figure 5 shows the overall trend for all binders combined. The difference between the binder types is relatively small.

The correlation could possibly be improved by considering unreacted CaO in the SCMs and the cement clinker (degree of hydration). However, this information is not available in most cases. It has to be considered that repeatability and reproducibility of the test itself contribute to the scatter (see [51] and Sect. 2).

3.2 Correlation between carbonation and binder content

Previous studies have indicated that the binder content of concretes (or mortars) has no systematic effect on the carbonation resistance of the materials, or that carbonation rate may even slightly increase with increasing binder content [55, 62, 63]. Nevertheless, the binder content was investigated as an influencing factor, since mixes with higher binder contents may offer a higher CO_2 buffer capacity. It is important to remark that the present analysis predominantly involves concrete mixes, with only a limited focus on mortar mixes.

A first analysis of mixes exposed to a natural indoor (controlled) environment showed no

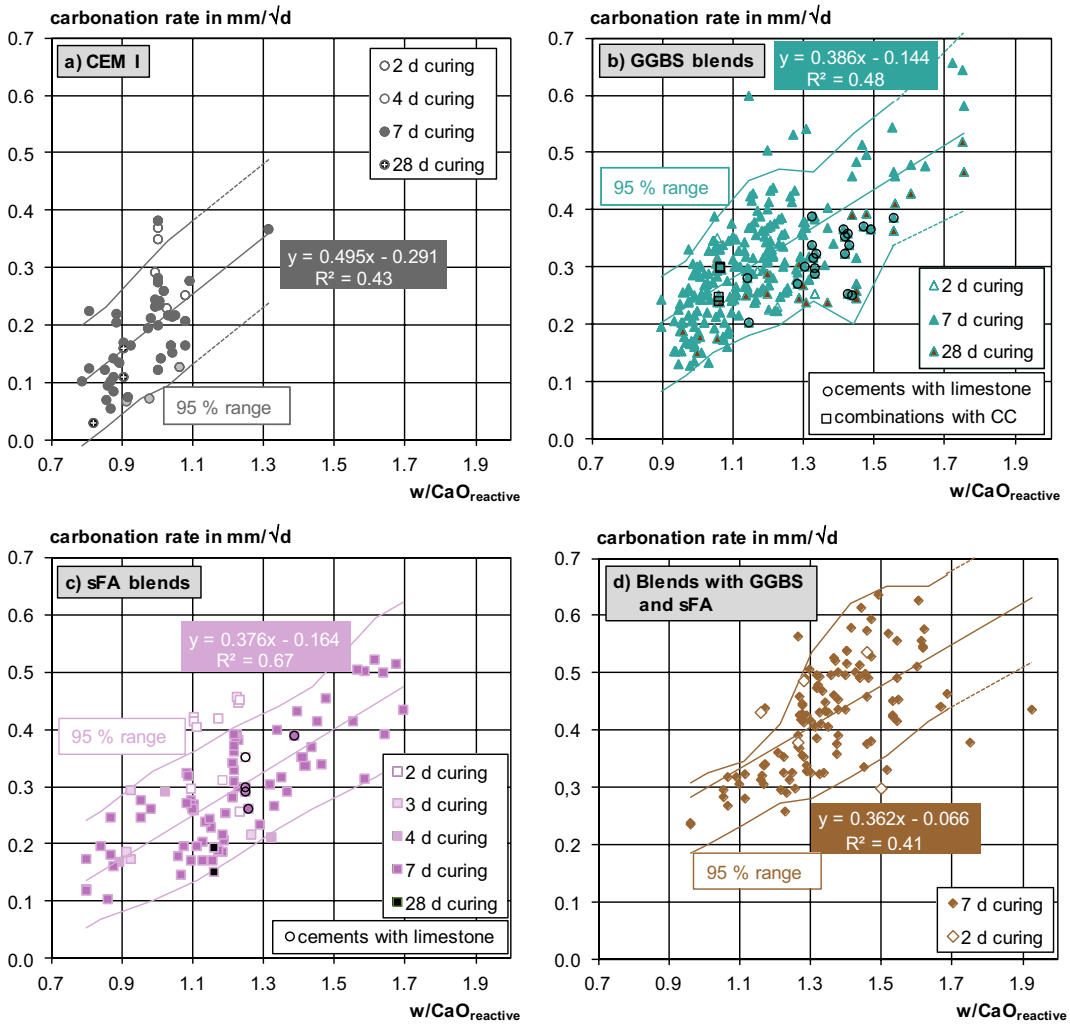

Fig. 4 Carbonation rate vs. w/$CaO_{reactive}$ for natural carbonation at 20 °C and 60–65% RH for different binder types and curing times. The best fit line and 95% range apply for 7 d curing

significant relation between the binder content (in the range of 232–600 kg/m^3) and the corresponding natural carbonation rates (see Fig. S1 in the Supplementary Material). This is not surprising, since multiple influential factors such as binder type, w/b ratio and curing conditions are not considered in this analysis.

Consequently, the data were grouped in clusters based on the types of SCMs incorporated into the binder system (Fig. S2). This considered both the type of SCM blended into the cement and those added directly to the concrete mix. For example, mixes were assigned to the cluster "GGBS" when they were produced with concrete contained blast furnace slag cement (e.g., CEM III/B) or when GGBS was added to the concrete separately from the cement. The clusters can be classified in four main groups, namely those involving (i) GGBS, (ii) sFA, (iii) metakaolin and calcined clays of different kinds (MK and CC), and (iv) limestone powder (L). Several mixes contained more than one type of SCM, making them part of two of these main groups. The analysis only addresses SCMs with data availability across multiple binder content ranges and at least two independent data sources. Minor comments are made for the other SCMs, which are silica fume, natural pozzolan, calcareous fly ash, Linz-Donawitz (LD) slag and burnt oil shale, but no conclusive analyses for those cases are possible because lack of data. Section 8 explores

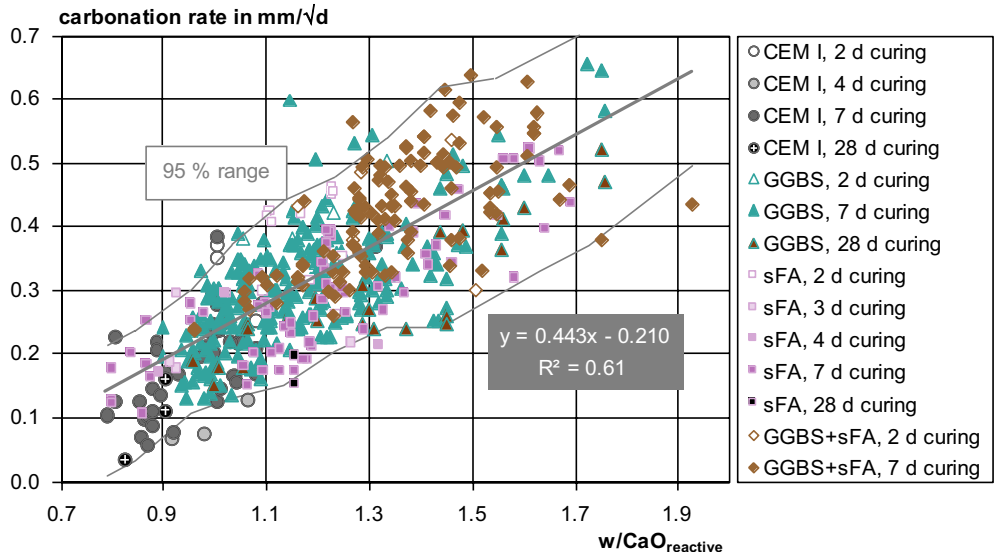

Fig. 5 Carbonation rate vs. w/$CaO_{reactive}$ for natural carbonation at 20 °C and 60–65% RH for all binder types and curing times. The best fit line and 95% range apply for 7 d curing

the effects of the SCM type and a method to address these in the global parameter $CaO_{reactive}$ content.

Due to the different nature of the SCMs, the ranges of the replacement ratios of the SCMs incorporated in the mixes are different, but for each of them relatively independent from the total binder content of the concrete mixes. In general terms, binder systems containing GGBS have replacement ratios in the majority of the cases ranging from 30–75%. In contrast, the most observed replacement levels for L, sFA, and MK & CC are 15–30%, 20–50%, and 10–35%, respectively. When combinations of SCMs are used, the resulting ranges fall intermediate to those of the individual composing SCMs. This variance in SCM content has an obvious impact on the alkaline reserve of concrete and affects the carbonation resistance of concrete.

Figure 6 shows the carbonation rates of concretes *versus* binder content for the different SCM types, and Fig. 7 presents a similar analysis with the more limited data for the mortar mixes. No clear trends can be observed in the figures, due to the effects of multiple factors which add up to the effects of the content and type of binder on the carbonation rate. The present data thus confirms that for the cement and SCM types under consideration, the binder content is, on its own, a poor predictor of the carbonation rate of concrete.

The binder content of concrete or mortar can also be expressed as aggregate to binder (a/b) volume ratio. To calculate this ratio, an air content of 2% (e.g., as indicated in ACI 211 for conventional concrete when maximum aggregate size is 20 mm) was assumed for all mixes and the volume of admixtures neglected in the present analysis. When only considering the natural (controlled) indoor exposure, a/b ratios ranged from 2.54 to 9.45. The SCM clusters described above were again considered to distinguish potential trends for the natural carbonation coefficient as a function of the a/b ratio (Fig. 8). For CEM I and sFA, an increase of carbonation rate with a/b might be discerned; however, the scatter of the data is large, and thus no significant correlation can be deduced from the data. For all other clusters, the data does not indicate a relationship between carbonation rate and a/b. Thus, the present analysis, which used natural indoor carbonation data, confirms and extends the previous studies [62, 63], which were based on accelerated carbonation testing.

3.3 Correlation between carbonation and compressive strength

Figure 9 shows the distribution of the replacement levels of Portland cement (SCM content) *versus* compressive strength, categorized according to the

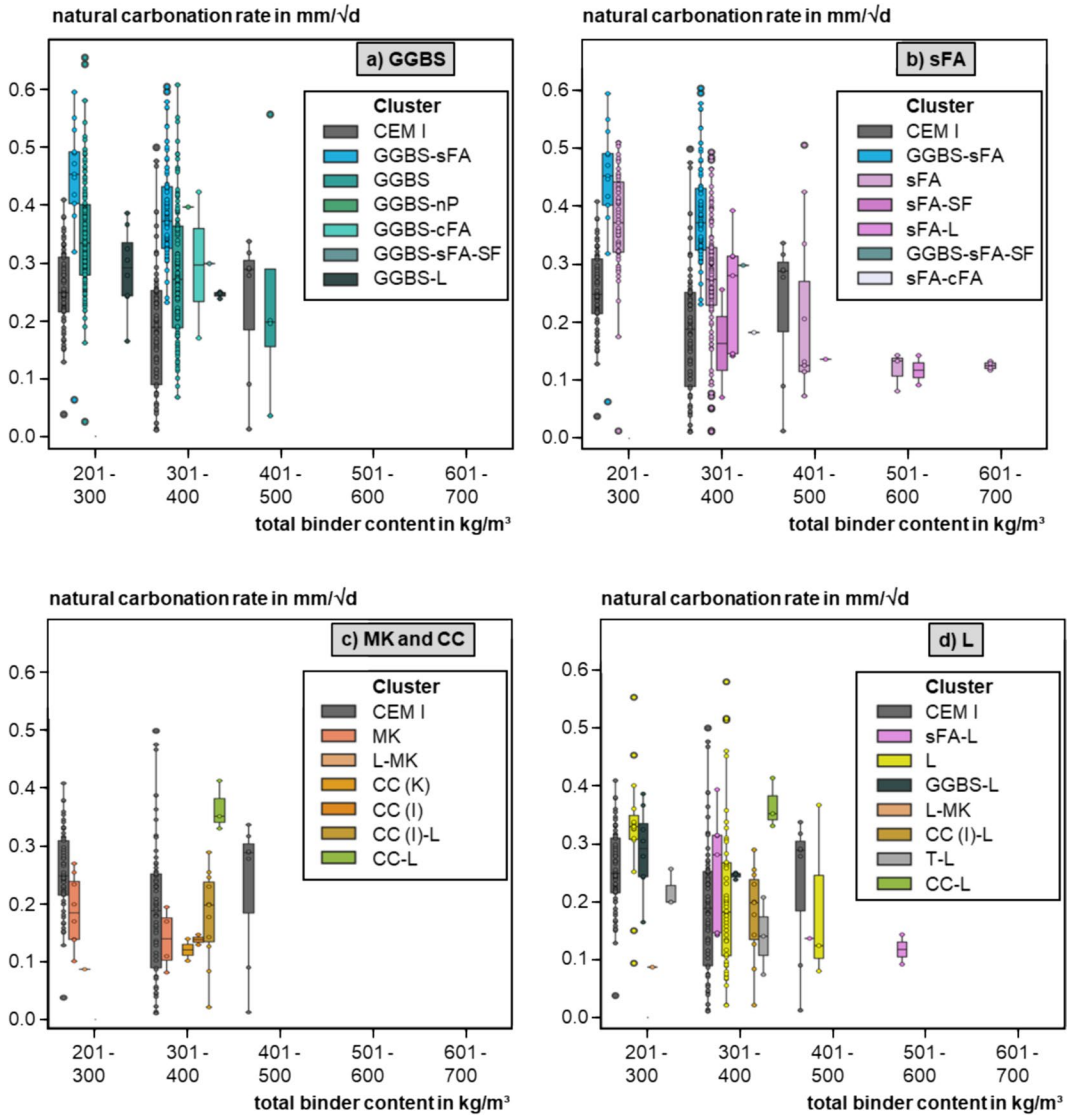

Fig. 6 Natural carbonation rate as a function of the binder content range for the various clusters including: (**a**) GGBS; (**b**) sFA; (**c**) MK and CC; (**d**) L in concrete mixes

different SCMs as in Sect. 3.2. Interestingly, comparatively high SCM contents were reported not only for the lowest compressive strength but for compressive strengths of 50–60 MPa and higher values too. This group comprises almost exclusively mixes from GGBS clusters, and a few cases from sFA clusters. From a sustainability and material efficiency standpoint, this suggests that concrete mixes with compressive strength levels below 40 MPa are not fully utilizing the hydraulic activity of CEM I. Sometimes, performance requirements in terms of workability or durability may limit the maximum content of some particularly challenging SCMs. However, for many other cases, opting for higher SCM content ratios than those mostly reported in the literature could be beneficial. This approach could leverage the properties of SCMs more effectively, contributing to the development of more sustainable and efficient concrete mixes.

The effects of the investigated SCMs on the natural carbonation rate reveal several insights when examined in function of the corresponding compressive

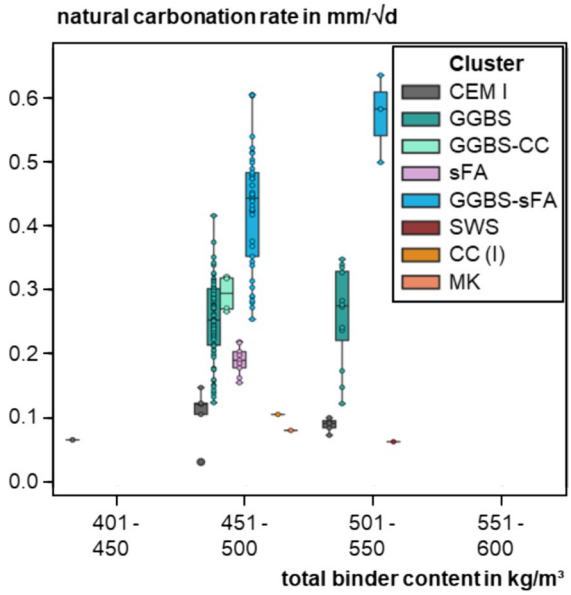

Fig. 7 Natural carbonation rate as a function of the binder content range for the various clusters in mortar mixes

strength (Fig. 10). For GGBS, sFA and L, there is a trend of decreasing carbonation rates with increasing compressive strength. The same trend may be discerned for MK and CC, although in this case the relationship is less clear. The general correlation between carbonation rate and compressive strength can be easily rationalized by considering that higher SCM contents lead to a higher $w/CaO_{reactive}$ and, thus, to a higher carbonation rate (Sect. 3.1), while at the same time higher SCM contents can also be expected to cause lower compressive strength. However, the latter relation is not universally true (Fig. 9), which partly explains the considerable scatter of the data and the fact that the correlation between carbonation rate and compressive strength is not significant. On the other hand, it is clear that a higher water content leads to a higher $w/CaO_{reactive}$ and thus to a higher carbonation rate, while it also results in a lower compressive strength.

As mentioned above, the plot for MK and CC (Fig. 10c) does not exhibit a clear correlation between

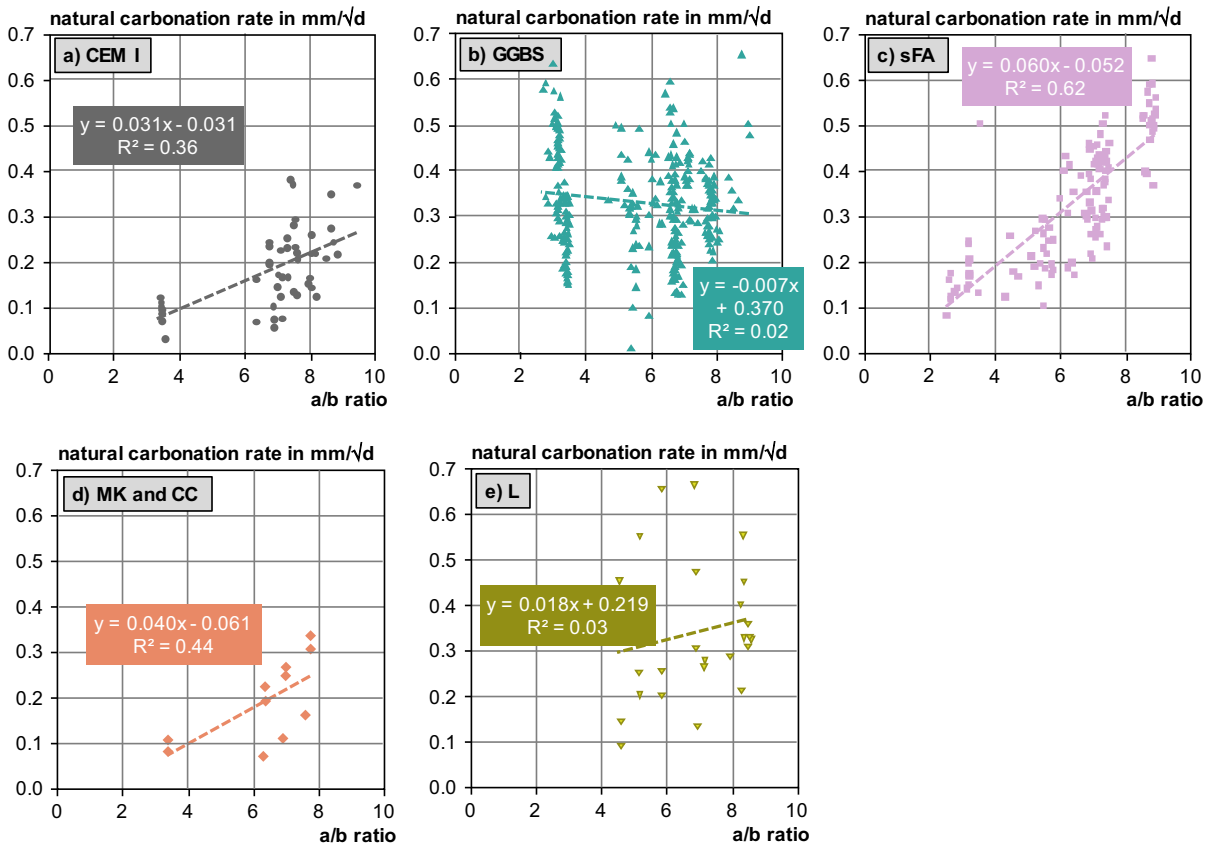

Fig. 8 Natural carbonation rate (indoor, controlled) versus a/b ratio

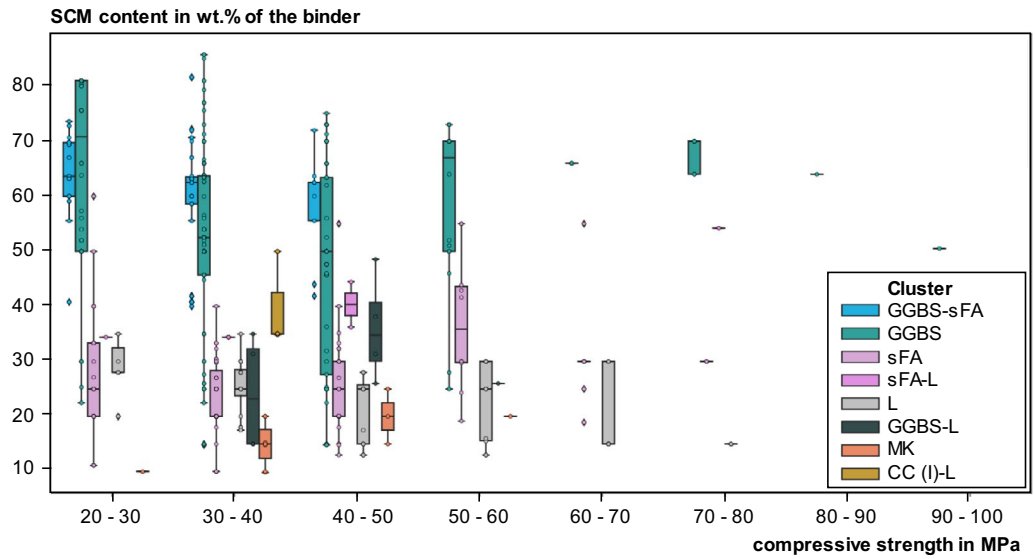

Fig. 9 SCM content versus compressive strength level (28 d strength, 150 mm cubes) *Note: For better clarity, the clusters with less than 7 mixes were neglected*

carbonation rate and compressive strength. This can be partly assigned to the fact that less data are available in the present database for concretes and mortars with MK and CC. In addition, it is well-known that MK and different CCs differ widely regarding their contribution to compressive strength as well as their influence on the durability parameters of the resulting materials (see, e.g., [37]), which likely also contributes to the considerable scatter and the absence of a clear trend.

When we think of $w/CaO_{reactive}$ as the parameter that controls the carbonation resistance, then the analyses from Sects. 3.1 and 3.2 can be conveniently combined with clustering based on the $w/CaO_{reactive}$ parameter. Unfortunately, the dataset is not balanced, and the MK and CC are not well represented. Therefore, the joint analyses of $w/CaO_{reactive}$ along with the total binder content or strength class excludes data for MK and CC, i.e., all clusters mentioned in Figs. 6 and (Fig. 10(c)). along with the other clusters with limited data (i.e. silica fume, natural pozzolan, calcareous fly ash, Linz-Donawitz (LD) slag and calcined burnt oil shale). Figure 11 shows corresponding plots to those presented earlier: natural carbonation rate versus (a) total binder content or (b) compressive strength, but with the clustering based on the $w/CaO_{reactive}$ (value intervals of 0.1 within the range [0.6–2.0]), instead of the type of SCM. Since the binder provides the buffering capacity in concrete and the water is the main driver for porosity, $w/CaO_{reactive}$ is related to the total binder content and the compressive strength correspondingly. Nevertheless, it is interesting to see to what extent the total binder content and strength class can be fully encompassed by the $w/CaO_{reactive}$ value.

In the ranges for which most data are available, 201–300 and 301–400 kg/m^3 for the total binder content (Fig. 11a), the natural carbonation rate increases as the $w/CaO_{reactive}$ increases. In addition, for a given $w/CaO_{reactive}$ value data suggests that carbonation rate does not change significantly when the total binder content increases from the range 201–300 kg/m^3 to the range 301–400 kg/m^3. It could be assumed that the trend maintains for higher total binder contents, but the data are not sufficient to support this statement. Therefore, at least for the case of GGBS, sFA, L, and CEM I, the dominant influence of the total binder content on carbonation rate seems to be limited to the provision of $CaO_{reactive}$ in concrete.

In Fig. 11b the lack of data for higher strength values is logical since only low mixing water contents are possible for such strength classes (i.e., high $w/CaO_{reactive}$ are incompatible with high strength classes). For a given compressive strength class, the carbonation rate increases as $w/CaO_{reactive}$ increases (Fig. 11b). However, for a given $w/CaO_{reactive}$ value the carbonation rate consistently decreases as the compressive

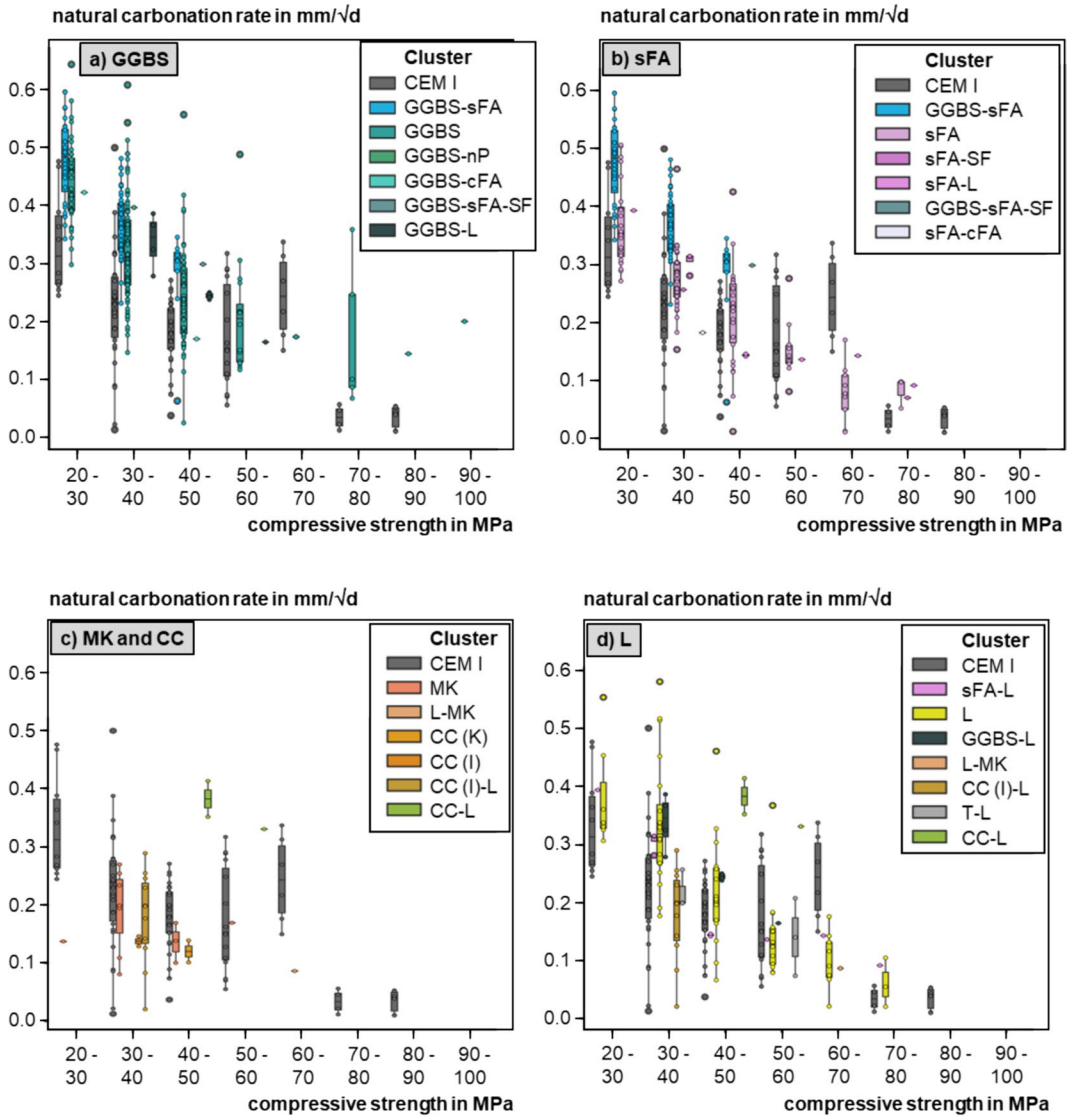

Fig. 10 Natural carbonation rate versus range of compressive strength (28 d, 150 mm cubes) for the various clusters: (**a**) GGBS; (**b**) sFA; (**c**) MK and CC; (**d**) L

strength increases from 20 to 60 MPa. It is unclear whether this is due to the non-linear correspondence between porosity and compressive strength or to some other factors affecting the natural carbonation rate that are not fully captured by the $w/CaO_{reactive}$.

4 Correlation between natural and accelerated carbonation

In accelerated carbonation testing, concrete or mortar specimens are exposed to an atmosphere with a CO_2 concentration that is higher than the natural CO_2 concentration in air (~0.04%). This serves to accelerate the carbonation of the cement matrix and obtain carbonation coefficients in a shorter time period than what is possible with natural carbonation testing.

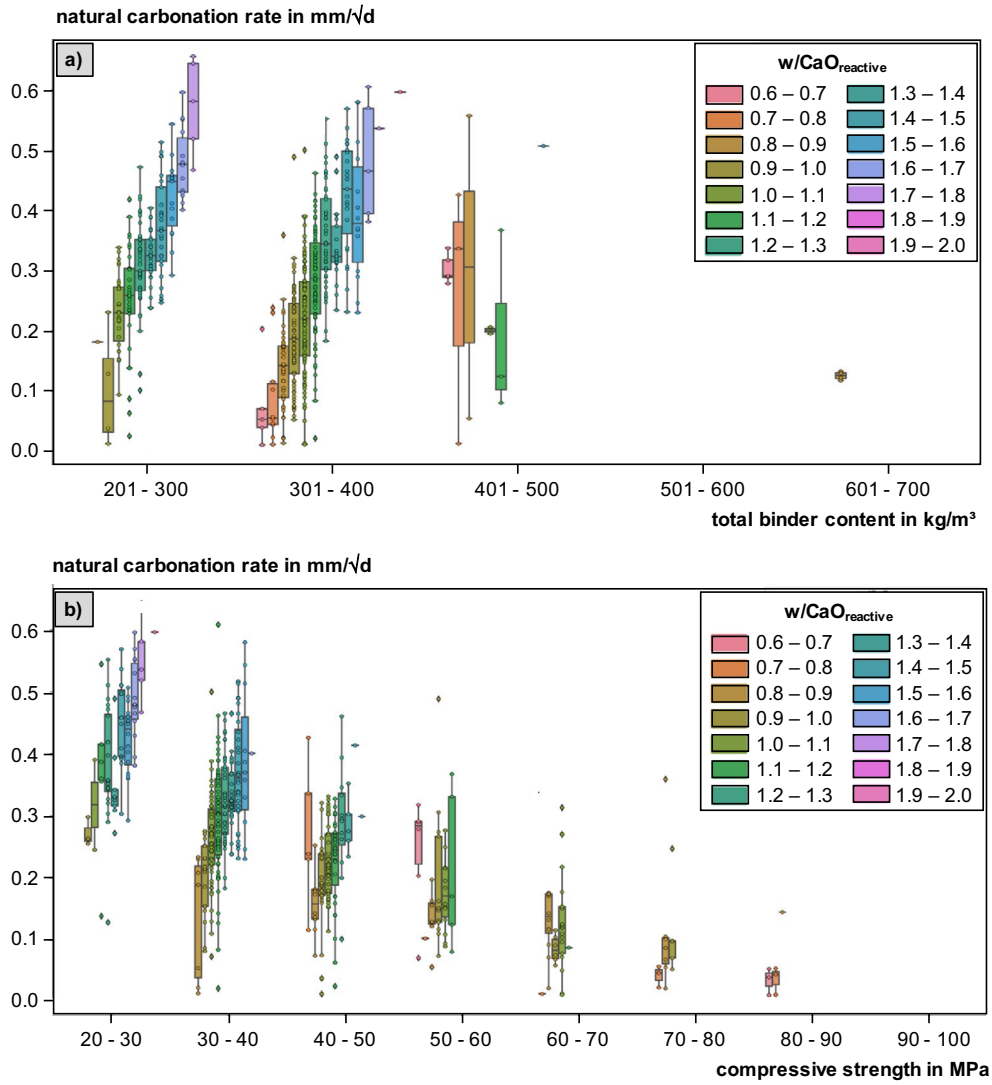

Fig. 11 Natural carbonation rate versus range of (**a**) total binder content and (**b**) compressive strength range (28 d, 150 mm cubes) for clusters based on $w/CaO_{reactive}$

Because of the increased CO_2 concentration in accelerated testing, the measured carbonation rates differ from the rates that would be determined for the same material under natural conditions. Thus, the rates need to be converted to obtain an estimate of the natural carbonation rates. This is often done with the square-root-of-time law, which is based on Fick's first law of diffusion [55, 64–66]:

$$\frac{k_{c,nat}}{k_{c,acc}} = \sqrt{\frac{c_{CO2,nat}}{c_{CO2,acc}}} \tag{5}$$

where $k_{c,nat}$ is the carbonation rate at the natural CO_2 concentration $c_{CO2,nat}$, and $k_{c,acc}$ is the carbonation rate measured at the increased CO_2 concentration $c_{CO2,acc}$.

For example, inserting 0.04% for $c_{CO2,nat}$ and 1% for $c_{CO2,acc}$ yields $k_{c,nat}/k_{c,acc} = \sqrt{(0.04/1)} = 0.2$. Strictly, the equation is only applicable when a similar microstructure and water saturation degree is achieved before exposure (referring to similar curing and preconditioning conditions) and when exposure conditions such as relative humidity and temperature are the same in both accelerated and natural carbonation testing. Some previous studies obtained data

supporting at least an approximate validity of Eq. (5) for blended cement concretes and mortars [33, 66], while significant deviations between predicted and measured natural carbonation rates have been noted in other studies of such materials [31, 55, 67, 68] as well as low-Ca alkali-activated concretes [69], generally indicating lower predicted natural carbonation rates based on accelerated carbonation testing than rates measured at natural CO_2 concentration.

For the present analysis, carbonation rates obtained under accelerated conditions were converted to a predicted natural carbonation rate through Eq. (5), assuming a natural CO_2 concentration of 0.04%. The values thus obtained were then compared to carbonation rates obtained under natural conditions for the same materials (Fig. 12). The natural carbonation rates of Durán-Herrera et al. [17] were determined in an "industrial environment" with the CO_2 concentration given as "0.02–0.09%". The present analysis indicates that the CO_2 concentrations in that study were, on average, significantly higher than 0.04%, and thus the application of Eq. (5) with $c_{CO2,nat} = 0.04\%$ to transform their accelerated (4% CO_2) carbonation rates yields predicted natural carbonation rates that are considerably lower than the rates determined under natural conditions. Using $c_{CO2,nat} = 0.09\%$ to calculate predicted natural carbonation rates from the accelerated carbonation data of Durán-Herrera et al. [17] yields predicted rates in the range 0.10–0.15 mm/$\sqrt{d}$; *i.e.*, the data would plot close to the lower boundary of the other data in Fig. 12. Nevertheless, as it is not known what the actual CO_2 concentration during the experiments of Durán-Herrera et al. was, it cannot be decided whether the latter plot corresponds better to the actual experimental conditions, and thus the data by Durán-Herrera et al. will be excluded from the following analyses.

However, also when ignoring the data by Durán-Herrera et al., it is apparent from Fig. 12 that the carbonation rates predicted from testing under accelerated conditions tended to be lower than the measured natural carbonation rates for $k_{c,nat} > 0.2$ mm/$\sqrt{d}$, and this trend became more pronounced with increasing $k_{c,nat}$.

The example of Durán-Herrera et al. demonstrates that carbonation testing under outdoor natural conditions is subject to more significant uncertainties than indoor testing under more strictly controlled conditions. To exclude extreme cases, Fig. 13 shows plots of the predicted natural carbonation rates *versus* measured natural carbonation rates only for the cases in which natural carbonation was conducted indoors. It was also checked whether the curing regime was similar for accelerated and natural indoor carbonation, which was not the case in 7 out of the 121 datapoints. This different curing seemed not to result in a significantly deviating relation between accelerated and natural carbonation, compared to equal curing prior to exposure (Fig. 13b). The plots in Fig. 13 are in accordance with the trend observed in Fig. 12 i e., the predicted natural carbonation rates were lower than the measured natural carbonation rates, and the absolute difference between these values increased with increasing $k_{c,nat}$. For accelerated carbonation testing at 1% CO_2, which is widely used and stipulated in standards for carbonation resistance testing (e.g., EN 13925), the number of available datapoints in the present database is comparatively low, and thus the trend was not as clearly apparent in the data (Fig. S3). Nevertheless, taken together, the results of the present analysis indicate that carbonation rates obtained under accelerated conditions are generally too low to accurately predict natural carbonation rates through application of the square-root-of-time law (Eq. (5)).

This observation is consistent with other practices and literature data. In the French national project PerfDuB [70], a good linear correlation was found between the experimental carbonation rates obtained under accelerated conditions (3% CO_2) and those obtained under natural conditions for a number of different concretes. A correlation factor of $k_{c,nat}/k_{c,acc} = 0.16$ was obtained. Thus, compared to the theoretical factor according to Eq. (5), $k_{c,nat}/k_{c,acc} = 0.12$, the experimental correlation factor was considerably higher. The difference between the two values was partly explained by the difference between the relative humidities applied under the different testing conditions ($50 \pm 5\%$ for natural carbonation, and 65% for accelerated carbonation). In order to take this discrepancy into account, an empirical model relating the carbonation rate to the relative humidity was used (see details in [70]), and a new theoretical factor was estimated at $k_{c,nat}/k_{c,acc} = 0.13$, which remains lower than the experimental correlation factor. Similarly, Swiss standard SIA 262–1 proposes a factor of 2.6 to convert accelerated

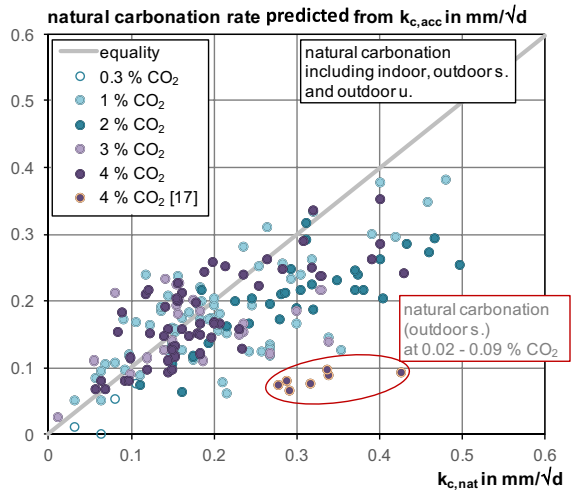

Fig. 12 Comparison of carbonation rates predicted using Eq. (5) and $c_{CO2,nat}=0.04\%$ from accelerated carbonation testing (CO_2 concentrations in the range 0.3–4%, as indicated in the legend), and measured carbonation rates determined under natural conditions, including indoor, outdoor sheltered (s.), and outdoor unsheltered (u.) conditions

carbonation rates (4% CO_2) in mm/√d to natural carbonation rates in mm/√a, while theoretically this factor would be $19.1\times0.10=1.91$. The factor 2.6 stipulated in SIA 262–1 appears to be based on measurements at natural CO_2 concentration and at 4% CO_2 respectively. The yielded carbonation rates obtained at natural CO_2 concentration were on average 1.36 times higher than carbonation rates computed from measurements at 4% CO_2 [71]. Finally, also the round robin on natural and accelerated carbonation testing, performed in the framework of RILEM TC 281-CCC [51, 52], revealed a similar behaviour, showing that the natural carbonation rate was underestimated by the accelerated carbonation rate (Table 2).

In addition to differentiating the data by CO_2 concentration or curing conditions (Fig. 13), also the binder type (Fig. 14) and *w/b* ratio (Fig. 15) was considered. Analogous to the previous figures, Figs. 14 and 16 only show the data related to indoor exposure. The majority of the different binder types available in the database approximately behave according to the expected relation based on Fick's first law (Fig. 14a). For GGBS, with $k_{c,nat}$ extending to ~ 0.5 mm/√d, a larger deviation of the relation between accelerated and natural carbonation from the line of equality can be observed (Fig. 14b). With respect to the *w/b* ratio, plotted in Fig. 15, no clear trend can be observed, except for the carbonation rates of materials with *w/b* = 0.45–0.50 and those with the highest *w/b* ratio

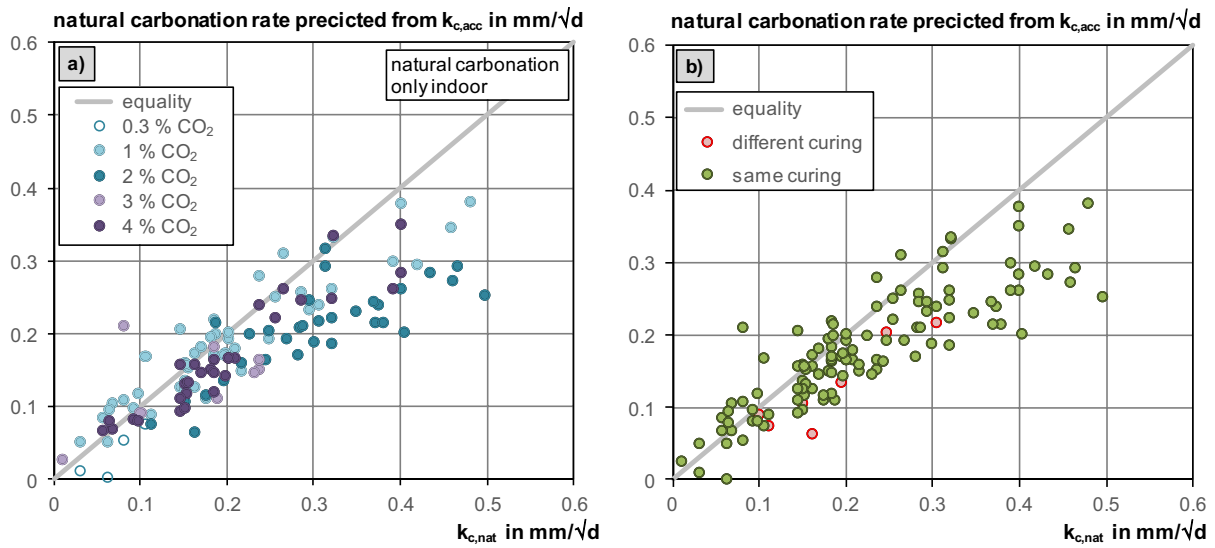

Fig. 13 Comparison of carbonation rates predicted using Eq. (5) and $c_{CO2,nat}=0.04\%$ from accelerated carbonation testing (CO_2 concentrations in the range 0.3–4%, as indicated in the legend), and measured carbonation rates determined under indoor natural conditions: (**a**) Colours of symbols indicating different CO_2 concentrations used in accelerated testing; (**b**) Colours of symbols indicating different or same curing conditions for natural and accelerated testing

Table 2 Ratio between natural and accelerated carbonation rates determined according to different international standards, compared to the theoretical ratio expected from Eq. 5 (data from [52])

Standard		EN 13295	fib	EN 12390–12	BSI 1881–210	SIA 262/1	LNEC E391	GB/T50082
CO_2 concentration		1%	2%	3%	4%	4%	5%	20%
theoretical $k_{c,nat}/k_{c,acc}$		0.20	0.14	0.12	0.10	0.10	0.09	0.04
	Mortar, indoor exposure	0.26	0.17	0.16	0.28	0.10	0.11	0.11
	Mortar, sheltered outdoor exposure	0.31	0.20	0.19	0.34	0.12	0.13	0.13
	Concrete, indoor exposure	0.27	0.22	0.15	n.d	0.13	0.10	n.d
	Concrete, sheltered outdoor exposure	0.33	0.27	0.19	n.d	0.17	0.13	n.d

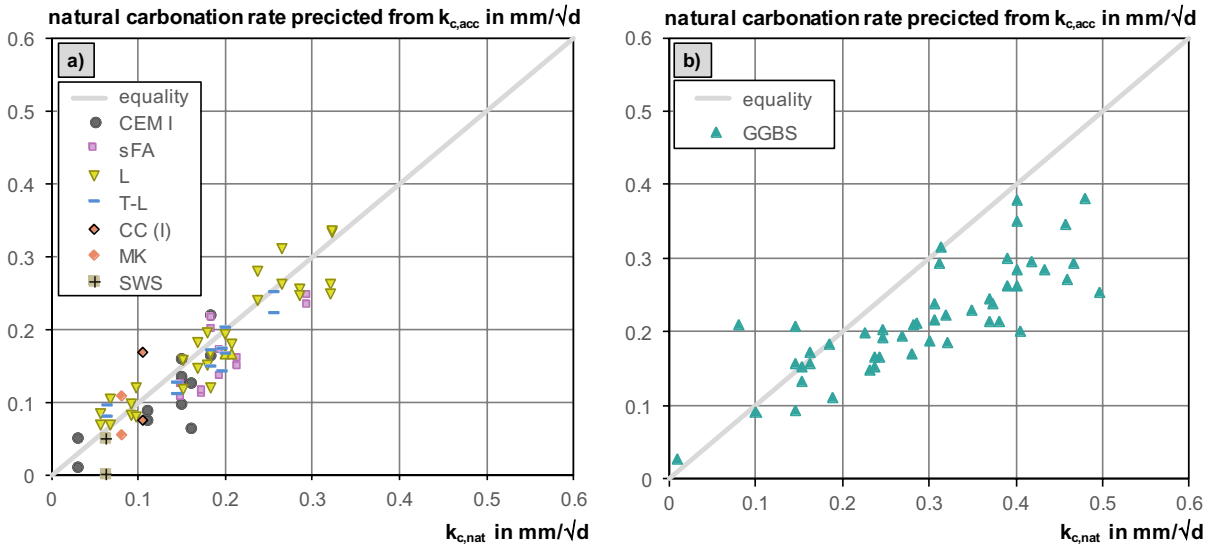

Fig. 14 Comparison of carbonation rates predicted using Eq. (5) and $c_{CO2,nat} = 0.04\%$ from accelerated carbonation testing (CO_2 concentrations in the range 0.3–4%), and measured carbonation rates determined under indoor natural conditions for different binder types: **a**): CEM I and binders with sFA, L, T, CC, MK and SWS; **b**): binders with GGBS

of 0.65, which deviate most from the expected theoretical relation. However, as these datapoints originate from only a few different studies, the plot and the former deviation might be biased.

Another way to examine whether there is a tendency of accelerated carbonation testing to yield predictions of natural carbonation rates that deviate from the carbonation rates obtained under natural conditions is to plot these rates together *versus* $w/CaO_{reactive}$ (Fig. 16a). The available data are in accordance with the above conclusion; namely, for all $w/CaO_{reactive}$ ratios higher than ~ 1.1 (corresponding approximately to $k_c > 0.2$ mm/$\sqrt{d}$), the carbonation rates predicted from accelerated testing, using Eq. (5) and $c_{CO2,nat} = 0.04\%$, tended to be lower than the measured natural carbonation rates. Notably, this trend is also clearly visible when plotting only the carbonation rates predicted from testing at 1% CO_2 together with the natural carbonation rates (Fig. 16b).

Possible reasons for deviations between the behaviour of concrete and mortar during natural and accelerated carbonation, particularly for high $w/CaO_{reactive}$, *i.e.*, for high water/binder ratios and/or high fractions of SCMs in the binder, have been reviewed

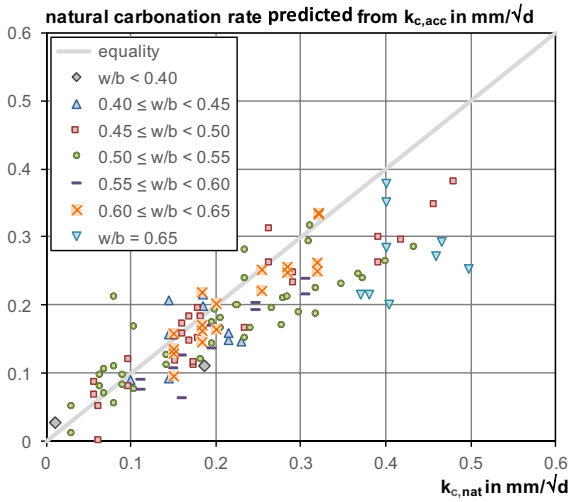

Fig. 15 Comparison of carbonation rates predicted using Eq. (5) and $c_{CO2,nat}$ = 0.04% from accelerated carbonation testing (CO_2 concentrations in the range 0.3–4%), and measured carbonation rates determined under indoor natural conditions for different w/b ratios

and discussed in a previous report by the present TC [55]. This review has highlighted that the phase assemblages and the chemical compositions of the pore solutions of OPC-based concretes and concretes with SCMs differ considerably, and that this has an influence on their carbonation rates. For example, aluminium provided by SCMs and incorporated into the C-A-S–H gel appears to alter the carbonation behaviour of that phase, compared to (virtually) Al-free C-S–H. It may be assumed that the magnitude of this effect may vary depending on CO_2 concentration, and thus may lead to different carbonation behaviour of concretes produced with and without SCMs at different CO_2 concentrations. In addition, while carbonation of OPC-based materials generally leads to densification of their microstructure, the carbonation of concretes with SCMs often leads to pore coarsening. Again, it might be conjectured that the strength of this effect could vary with CO_2 concentration, which would possibly provide an explanation for the observed deviations between the behaviour of concretes with low and high $w/CaO_{reactive}$ at different CO_2

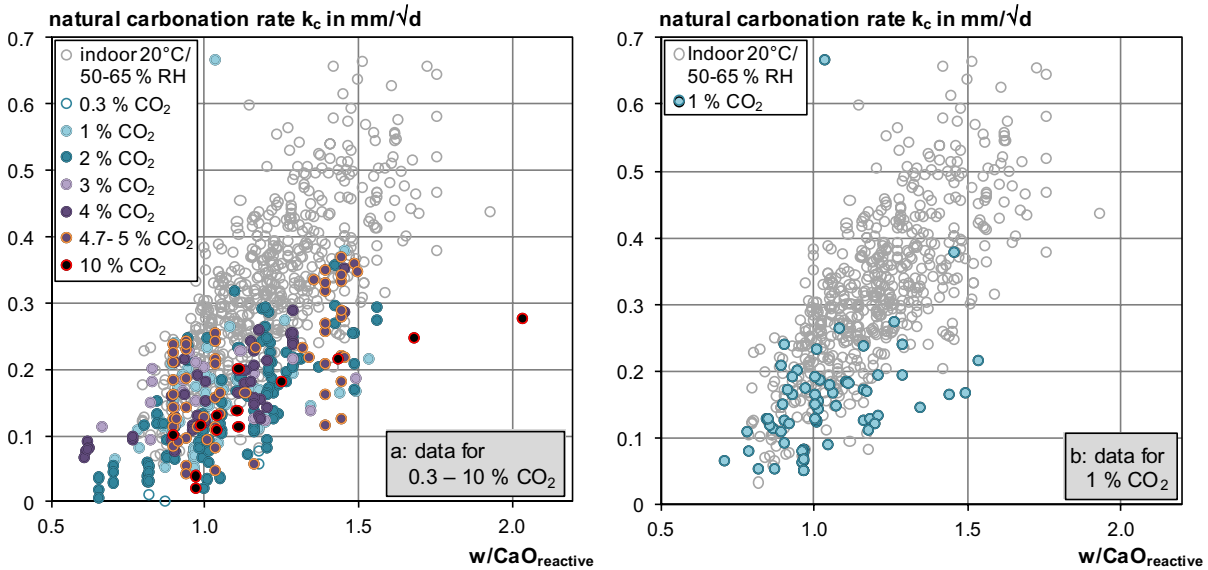

Fig. 16 Predicted and measured natural carbonation rates vs. $w/CaO_{reactive}$. Grey empty circles represent data obtained under indoor natural conditions, and filled circles represent carbonation rates predicted from accelerated testing (left: CO_2 concentrations in the range 0.3–10%, right: data for 1% CO_2) and application of Eq. (5) with $c_{CO2,nat}$ = 0.04%. *Note: The datapoint at (1.036; 0.667 mm/√d) has been obtained for a concrete produced from an OPC which was apparently highly pre-hydrated and a GGBS with an untypical mineralogical composition, with a comparatively low 28-day strength of 16.3 MPa and massive strength deterioration during accelerated carbonation* [1]*; it is thus not representative of concretes as usually applied in civil engineering*

concentrations. Additional peculiarities of materials with SCMs that may be connected to the observed deviations concern the rate of carbonation of C–(A–)S–H, the relative amounts of $CaCO_3$ formed from C–(A–)S–H and portlandite, respectively, and precipitation of the different polymorphs of $CaCO_3$ [55] as well as possible effects of the water produced by carbonation of portlandite and C–(A–)S–H [67].

5 Effect of curing on carbonation under natural and accelerated conditions

It is well known that curing affects carbonation [55], and its effect is widely discussed in the literature. Saillio, [72] as well as Gruyaert et al. [22] and Bertin [73] showed that increasing the curing time slows down the subsequent kinetics of carbonation. The intensity of this effect depends on the type of the SCM used in the binder. This decrease in carbonation kinetics can be explained by the increase in the degree of hydration which increases the quantity of phases that are amenable to carbonation and decreases the diffusion coefficient of CO_2 in the material. Rozière [74] showed that curing through storage in water for 28 days led to significantly higher carbonation resistances than leaving the samples in formwork for the same period of time. Buenfeld et al. [75] showed in their investigations of concretes aged for 120 days that the effect of the types of curing regime on the durability properties is significantly lower compared to the duration of curing. The present database was therefore used to analyse the effect of the curing duration on carbonation. Of the 1044 data sets in which systematic information on curing was available, the curing duration of 7 d was the most frequently represented with 727 data sets. In addition, data on 1 d, 2 d, 3 d, 4 d as well as longer curing times of up to 112 d are available. Since 7 d curing was the most frequent, it was chosen as the reference curing period. In Sect. 3.1, Figs. 4 and 5 already confirm that curing for less than 7 days leads to significantly higher carbonation rates probably due to higher porosity in a less mature structure.

Figure 17 shows the relative carbonation coefficient versus the curing duration for mixes with different compositions under natural carbonation. Here, the effect of curing on natural carbonation seems to present some dependency on the type of binder: the effect of curing on mixes having higher SCM and lower clinker content results in faster carbonation rates.

The effect of curing duration is shown in Fig. 18 for the concrete compositions with CEM III carbonated under natural and accelerated conditions. Note that the effect of increased curing duration is significantly more pronounced under accelerated conditions compared to the natural ones. Figure 19 displays the effect of curing for concrete mixes with CEM I under natural outdoor conditions. Both best fit up to one year and best fit for longterm (here 13 years) were compared. Longer exposure times obviously led to an increased influence of curing time (doted lines in Fig. 19).

Thus, the curing duration, particularly for curing times up to 7 days, has a decisive effect on the progress of carbonation over time. The data analyis showed that the the effect of curing strongly depends on the carbonation conditions and is less pronounced for natural carbonation. A very long curing time could therefore even compensate for a strong reduction in the clinker content, but current construction practices and standards leave few possibilities to exploit this potential.

6 Effect of relative humidity during pre-conditioning on carbonation

The pore structure and in particular its degree of saturation influences the progress of carbonation [76]. It is therefore expected that the outer relative humidity during pre-conditioning and its duration also affect the carbonation rate as it affects the evolution of the microstructure. However, since only a few studies are available in the database, a systematic evaluation is difficult.

In several accelerated carbonation standards like EN 12390–12, no criteria are specified for relative humidity during pre-conditioning. The new French standard for accelerated carbonation XP P18-458 requires preconditioning in two stages. The first stage consists of drying the samples at 45 °C for at least 14 days in order to reduce the saturation degree of the studied mortar or concrete, thus increasing the carbonation kinetics. Then, there is a second step which consists of storing at 20 °C and 65% RH for 7 days in

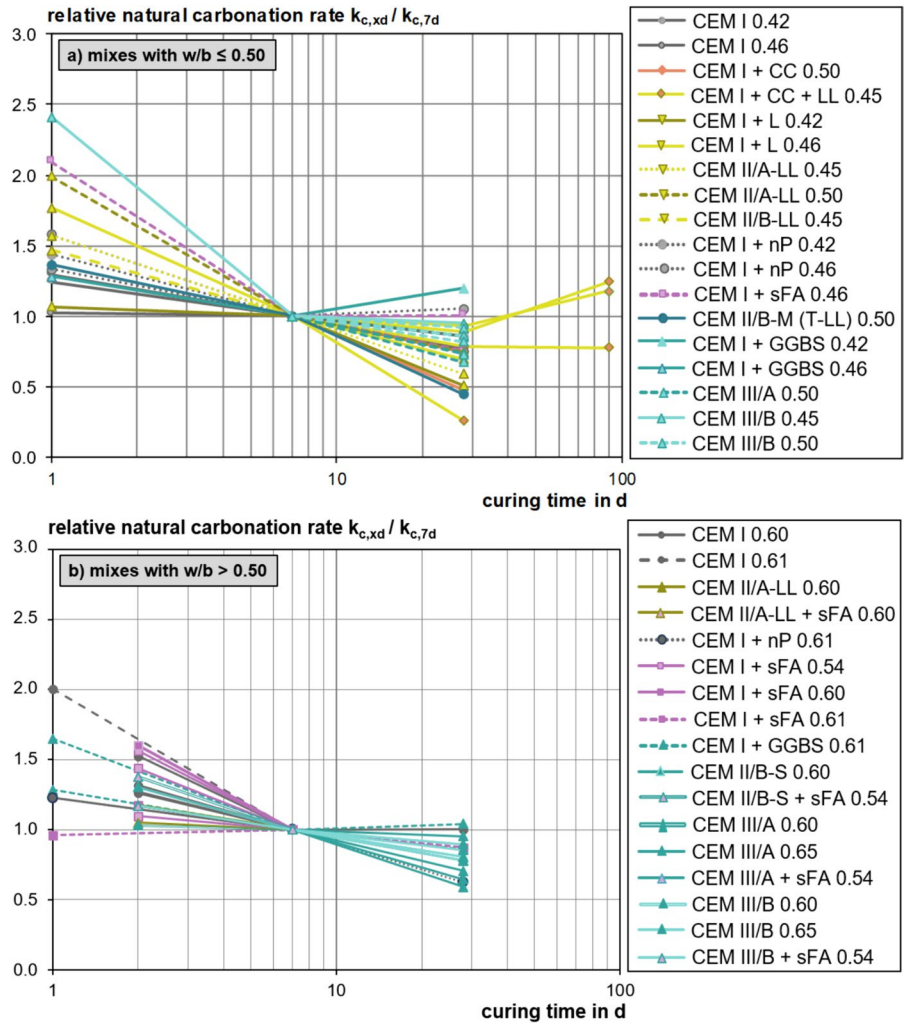

Fig. 17 Relative carbonation coefficient $k_{c,xd}/k_{c,7d}$ versus curing duration for mixes with different composition exposed to natural carbonation *Note: Same labelling for different results can be derived from the fact that the labelling only mentions binder type and w/b value but other parameters were also varied (for example different studies could have used similar compositions or further parameters were varied such as the SCM content)*

order to cool the samples. More details on the development of this preconditioning can be found in [70].

Forsdyke and Lees [77] evaluated the effect of preconditioning on the rate of carbonation. Four different curing regimes were applied. Specimens were either cured under water or held in laboratory conditions (an environment of 20±2 °C and 60±5% RH) for 14 days. Additionally, speciments were cured under water or in laboratory conditions for 11 days and then oven-dried (105 ^{0}C and low RH) for 3 days. Oven-drying before carbonation led to slightly increased carbonation rates for the water cured samples (less than 1 mm difference). However, oven-drying on air-cured samples led to lower carbonation rates. The authors do not give a reason for this beaviour but refer to further literature which shows the effect of oven-drying on the alteration of the micro-structure of concrete. The high temperatures during oven preconditioning, such as 105 ^{0}C used in this case, can remove both free and physically bound water from concrete (dehydration of gypsum begins around 80 °C and decomposition of ettringite begins around 60 ^{0}C, leading to chemical changes). Furthermore, since carbonation reactions take place in concrete pores and rely on the presence of an optimal amount of pore water, the RH during preconditioning may also alter the carbonation behaviour of concrete.

To conclude, the relative humidity during preconditioning also affects the carbonation rates and needs to be further studied; there are not yet enough data in

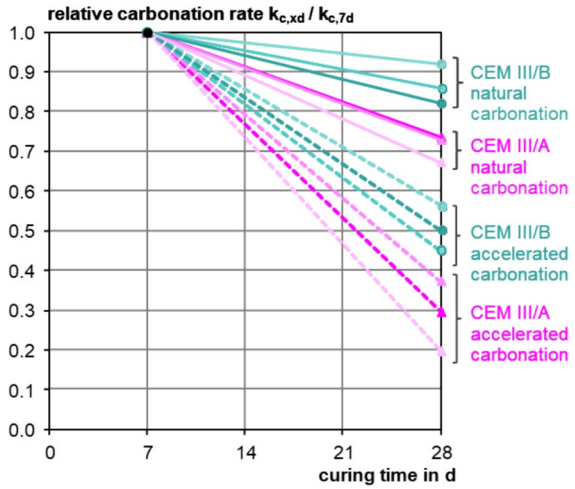

Fig. 18 Relative carbonation coefficient $k_{c,xd\ curing}$ / $k_{c7d\ curing}$ versus number of curing days for mixes with same composition exposed to natural (solid lines) and accelerated (dashed lines) carbonation

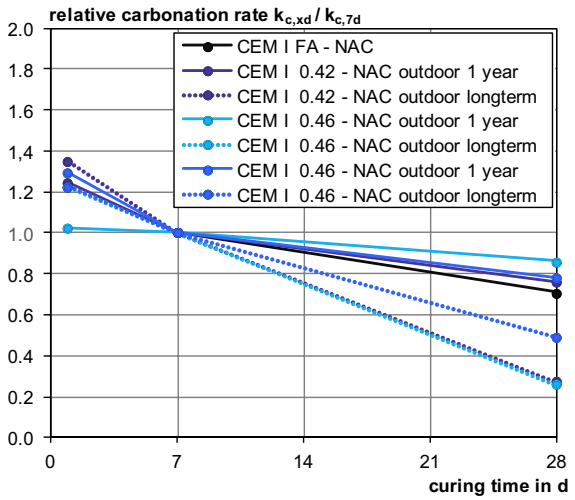

Fig. 19 Relative carbonation coefficient $k_{c,xd}/k_{c,7d}$ versus number of curing days for mixes with the same composition exposed to natural carbonation (data from [35])

the database to systematically investigate the effect. Here, systematic studies under an inert gas atmosphere to separate the effect of drying from carbonation would be interesting, see also [78, 79].

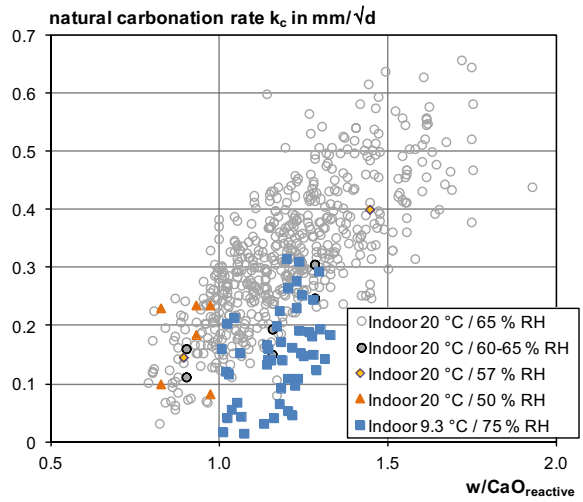

Fig. 20 Carbonation rate vs. w/$CaO_{reactive}$ for indoor natural carbonation at different temperatures and relative humidities (RH)

7 Effect of relative humidity during carbonation under natural and accelerated conditions

The relative humidity of the atmosphere during carbonation affects the degree of saturation of the pore system of concretes and mortars with water (pore solution). This, in turn, has an influence on the diffusion of CO_2 into the concrete and the kinetics of the reaction of CO_2 with the cement paste, and thus on the rate of carbonation. Early work found that the pessimum RH, *i.e.*, the RH at which the carbonation rate is at its maximum, is ~ 60% (e.g. [80]). A RH close to this value has been stipulated in several standards on carbonation resistance testing of cementitious materials. However, it has been noted that the pore size distributions, and how these are altered during carbonation, differ between Portland cement-based materials and materials based on blended cements. Materials with blended cements tend to have a finer pore structure than those with CEM I and therefore have a higher degree of saturation at the same RH [31, 79]. In addition, the various cement hydrates exhibit different carbonation behaviour, and this behaviour clearly depends on RH (for example, whether portlandite is completely consumed during carbonation) [61], while materials based on CEM I and blended cements generally exhibit different relative abundances of the major cement hydrates. Therefore, the

relationship between RH and carbonation rate may be different for the two classes of materials.

For natural carbonation testing performed indoors, *i.e.*, under controlled temperature and RH, most of the measurements in the present database relate to testing at 20 °C and 65% RH, while fewer data are available for other conditions. A plot of the corresponding carbonation rates versus $w/CaO_{reactive}$ (Fig. 20) does not indicate a significant deviation of the data obtained at 20 °C and RHs of 50%, 57%, and 60–65% (*i.e.*, less strictly controlled) from the data determined at 20 °C / 65% RH. Measurements performed at 9.3 °C / 75% RH for concretes produced with GGBS-containing cements [19] yielded considerably lower carbonation rates than measurements at 20 °C / 50–65% RH (Fig. 20, Figs. S4 and S5). However, since in the latter dataset both the temperature and the RH were significantly different from those in the other measurements, and the effects of these two parameters are difficult to disentangle without additional information, [1] this dataset will be excluded from the further analysis.

For the following comparison of the indoor carbonation rates with the outdoor carbonation rates, an additional dataset, for which the report notes that outdoor carbonation was conducted in an "industrial environment" with CO_2 concentrations in the range 0.02–0.09% [17], was also excluded, as these conditions gave unusually high carbonation rates, compared to the rates that were obtained presumably at

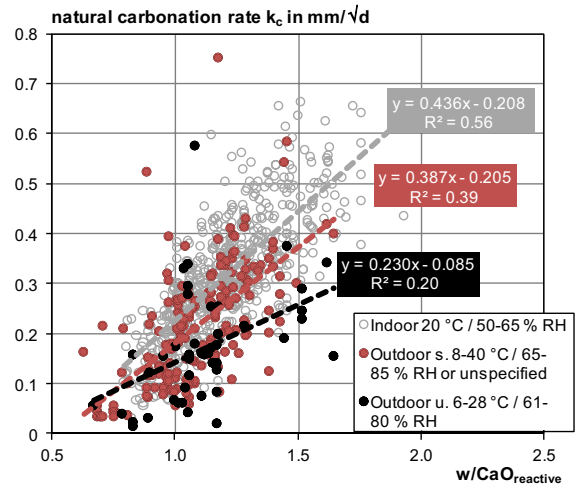

Fig. 21 Carbonation rate vs. $w/CaO_{reactive}$ for natural carbonation rates of concretes obtained indoor at 20 °C/50–65% RH, outdoor sheltered (s.), and outdoor unsheltered (u.)

CO_2 concentrations of about 0.03–0.04% (Fig. S6; cf. Section 4).

A plot of the remaining data (Fig. 21) shows that the scatter of the outdoor data was higher than that of the indoor data, and it indicates that outdoor testing, particularly under unsheltered conditions, yielded lower carbonation rates than indoor testing. This observation holds true even when suspicious carbonation rate data, *i.e.*, carbonation experiments with an intercept of the carbonation depth-*versus*-time data (d_c at $t = 0$ d) larger than 2 mm or lower than − 2 mm, are removed from the analysis (Fig. S7). These findings can be explained by the aforementioned observation that a pessimum RH around 60% exists [80], which is close to the RH applied in indoor testing, while the RH under outdoor conditions is often significantly higher, and under unsheltered outdoor conditions rainwater can contribute to the saturation of the concrete pores [83–86], leading to lower carbonation rates.

For carbonation rates determined under accelerated conditions, the present database contains only data obtained at RH in the range of 55–70 %, distributed among several groups of measurements at different CO_2 concentration. Thus, for each CO_2 concentration, only carbonation rates determined at one or a few similar RH are available, and accordingly no clear correlation between carbonation rate and RH in accelerated carbonation testing could be identified in

[1] The carbonation rates obtained at 9.3 °C / 75% RH were smaller than the rates determined at 20 °C / 50–65% RH by a factor of approx. 0.5 (Supplementary Fig. S4). The diffusion coefficients for the inter-diffusion of gases can be derived to be proportional to T^n, with T being the absolute temperature and n in the range approx. 1.5–2.3, depending on the diffusing gases and the assumptions made to derive the relationship [81, 82]. Taking the highest exponent, $n = 2.3$, and ignoring any influence of RH for the sake of argument, the ratio of diffusivities in the two sets of experiments is calculated to be $(282.45\ K)^{2.3}/(293.15\ K)^{2.3} = 0.92$, which is considerably higher than the observed ratio of the carbonation rates of ~ 0.5. This indicates that the influence of temperature on the diffusion coefficients in the two testing conditions cannot fully account for the differences between the measured carbonation rates, and thus an influence of RH exists. However, the above calculation is only an estimate, and a quantitative evaluation of the relative importance of temperature and RH for the carbonation rates would require a more detailed analysis.

the present data (Fig. S8). The observed scatter of the data for each of the CO_2 concentrations and RH used in testing is likely caused, in part, by the differences between the methods of curing and preconditioning, as discussed in sections 5 and 6.

In summary, data that allow a systematic comparison of the influence of RH on the carbonation rate of a significant number of cementitious materials under otherwise equivalent conditions appear not to be available. Namely, in all examined studies, natural indoor testing was either performed at 20 °C and a RH in the range 50–65% RH (mostly 65%), or at a temperature that deviated significantly from standard conditions, while for accelerated testing only a few data are available for each CO_2 concentration and RH. Thus, the hypothesis that different pessimum RHs exist for different binders cannot be examined with the existing data. However, the present database shows that testing under conditions as specified in many standards (constantly ~ 20 °C and ~ 65% RH) leads to more conservative (i.e., higher) carbonation coefficients than testing under natural conditions with varying temperature and RH, i.e., outdoor testing.

Finally, Sect. 7 highlights the need for systematic studies on the effect of RH on the carbonation performance of different blended cementitious systems (having different degrees of saturation due to their varying pore structure). Furthermore, it is noted that the scatter of the measured carbonation rates was higher for outdoor testing than for indoor testing. Regular recording of the climatic parameters under outdoor conditions is therefore essential to interpret the measured carbonation rates correctly. In this context, it is noted that Huy Vu et al. [86] already showed that average climatic parameters do not fully explain the differences between the carbonation rates of concretes under real climate conditions in five different countries. In addition, the authors found that the number of rainy days per year, rather than cumulative rain (or average RH), is a suitable proxy for the effects of saturation of concrete pores on the reduction of the carbonation rate due to the alternate wetting and drying of the concrete surfaces. Furthermore, efforts should be made to evaluate the effects of the heterogeneous distribution of the internal relative humidity in concrete, governed by the presence of residual water and water vapour diffusion in cementitious materials, as highlighted by Steiner et al. [61].

8 Multiple variable analysis using probabilistic inference and machine learning

In the preceding sections, we individually analysed the primary factors impacting carbonation rates. In this section, we aim to undertake a collective analysis of all variables within the compiled dataset in two distinct ways. Firstly, from a physics-based perspective, addressing critical inference questions (Sect. 8.1) previously discussed separately; and secondly, from a machine learning standpoint, exploring the efficacy of estimating carbonation depth from these variables (Sect. 8.2). The data underwent preprocessing using state-of-the-art tools [87, 88] before any modelling exercises. This process culminated in a tidy data table [89] comprising 9359 rows and 39 columns, encompassing sample IDs, variables, and their measured properties.

8.1 Probabilistic inference

The model we consider here involves two equations: (i) Calculation of $CaO_{reactive}$ contents through the various binder components; (ii) Calculation of carbonation depth utilizing the outcomes of the former equation. A Bayesian approach, employing Markov chain Monte Carlo (MCMC) sampling via Stan, is employed to fit the parameters in both equations at once [90, 91]. The diagnostic potential scale reduction factor, $\hat{R}$, consistently approached one, indicating convergence of the MCMC chains.

In Sect. 3.1 the $CaO_{reactive}$ content was estimated on a sample basis, using the measured total CaO content of the binder and excluding phases that do not contribute to CO_2 binding (limestone and calcium sulfate phases, see Eq. 4). In this section, the average and standard deviation of the total CaO contents are calculated for each of the different binder components, the average is multiplied by 0.95 to account for the fact that not all CaO is reactive, based on the calculations in Sect. 3.1, and the resulting numbers are used to define normal prior distributions for the $CaO_{reactive}$ weight percentages. An exception is made for SCM type L, for which we assume that all CaO is non-reactive. This enables us to estimate the $CaO_{reactive}$ content when information on chemical composition is missing. For this purpose, Eq. 6 is used:

$$\mathrm{CaO}_{\mathrm{reactive}} = C \cdot W \tag{6}$$

where C represents the predictor matrix containing the quantities of different binder components, except SCM L, in kg/m^3, while W denotes the vector of weight percentages, serving as parameters in our model, delineating the relative amounts of $\mathrm{CaO}_{\mathrm{reactive}}$ in each binder component.

Next, we estimate the carbonation depth d_c through Eq. 7 which relates the carbonation depth to the main influencing parameters identified in previous sections:

$$\begin{aligned} dc \; &= a \cdot 10^{-bf_c} \cdot \left(1 - \frac{RH}{100}\right)^{c} \cdot \left[CO_2\right]_0^{\;d} \\ &\cdot t^{e} \cdot CaO_{reactive}{}^{-f} \cdot 10^{-977 \cdot g/T} \end{aligned} \tag{7}$$

where a, b, c, d, e, f, and g are inferred parameters, f_c is the compressive strength, RH is the relative humidity during carbonation, $\left[CO_2\right]_0$ the CO_2 is concentration at the surface, t is the time, and T is the temperature (in Kelvin) during carbonation.

Most factors in this product represent expressions that are often encountered in literature, for estimating carbonation depth [92–94], while the exponential of f_c is representing an estimate of the diffusivity of CO_2 (from CEB-FIP Model Code 1990, see *e.g.* [94, 95].), and the exponential of the inverse of T is based on the Arrhenius law, with 977 the ratio of the average apparent activation energy of the range mentioned by Li et al. [96] for concrete carbonation, to the universal gas constant, converted to base 10.

While the square root of time law is often assumed, deviations are observed (e.g. [94, 97]). To account for this, a deviation from square root behaviour is allowed by employing a double exponential prior distribution for parameters d, e, f, and g. This is a regularizing probability distribution, as most of the probability mass is concentrated around the square root behaviour, while if there is clear evidence in the data for deviations from square root behaviour, the posterior can move towards the tails of the double exponential prior. Gaussian priors centred at literature values are used for b [94] and c [93]. Additionally, a Gaussian likelihood is used for the carbonation depth, where the measurement error is modelled as a combination of two parts: an absolute and a relative error. For the former, we use a normal prior with a mean of zero and a standard deviation of 0.05, while for the latter, both the mean and standard deviation are set to 0.5. Both prior distributions are truncated at zero, to ensure that they remain positive.

This model aligns with the approach for predicting the carbonation rate mentioned in Sect. 2 but allows for deviations from the square root of time through parameter e. It accounts for the impact of $\mathrm{CaO}_{\mathrm{reactive}}$ quantity studied in Sect. 3.1, estimated from the individual binder components, and utilizes the CO_2 diffusivity estimate derived from measured compressive strength instead of water-related factors explored in Sect. 3.3. Merging of natural and accelerated experiments while considering CO_2 concentration at the surface ($[CO_2]_0$) is discussed in Sect. 4. However, certain factors such as curing (Sect. 5) and relative humidity during preconditioning (Sect. 6) are not included in this model, while they do account for relative humidity during carbonation, albeit not including a pessimum around 60% as suggested in Sect. 7.

The results of the model fitting are depicted in Figs. 22 and 23, illustrating varying levels of certainty in identifying weight percentages for the different binder components as well as the factor and different powers in the carbonation depth equation. Figure 23 additionally provides a posterior predictive check (subplot (d)) that aligns well with the data. The model demonstrates an adequate description of data with an observed mean absolute error of 1.33 and an R^2 of 0.82 for the maximum a posteriori (MAP) estimate, although it does seem that adding a positive intercept, potentially per sample, may help in fitting the small depths, as mentioned in Sect. 2. Notably, certain exponents deviate from square root behaviour; this is discussed in more detail in Sect. 8.3. Finally, the reactive CaO weight percentage for SCM GGBS seems rather low compared to the prior mean of about 40%. This seems to suggest that about one fourth of the CaO contents of GGBS may not contribute to CO_2 binding, presumably because the GGBS has not fully reacted prior to carbonation.

Finally, to gauge the variables' impact on carbonation depth, values of different factors in the equation were calculated using the MAP parameter set, as shown in Fig. 24. These distributions suggest that time of exposure, CO_2 concentration, compressive strength, $\mathrm{CaO}_{\mathrm{reactive}}$, relative humidity, and temperature, in that order, influence carbonation depth. Given the log scale, the width of these distributions provides an idea on the importance of the factors in determining the carbonation depth. It is noted, however, that

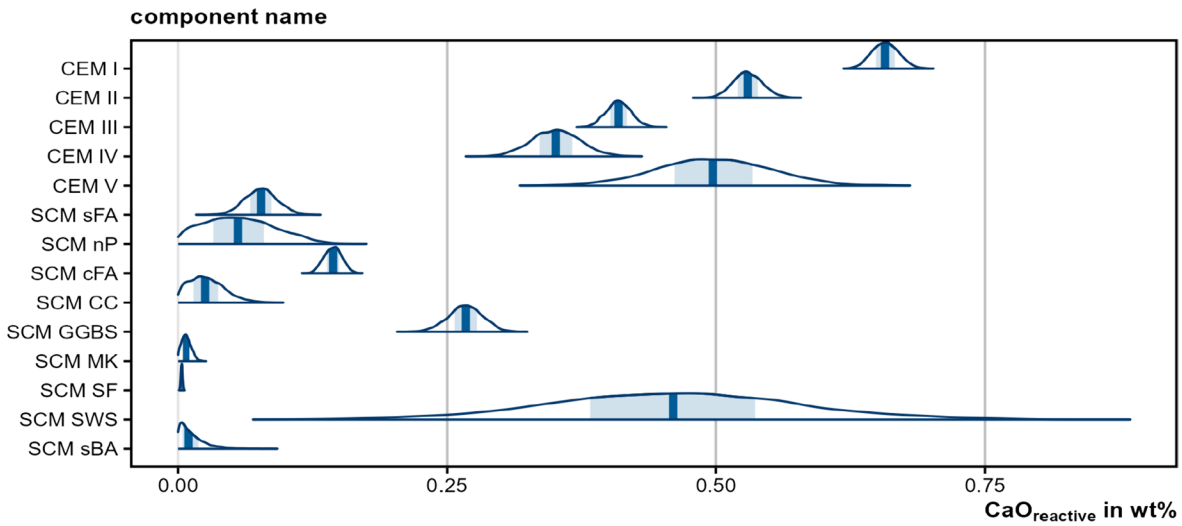

Fig. 22 Posterior distributions of the $CaO_{reactive}$ weight percentages

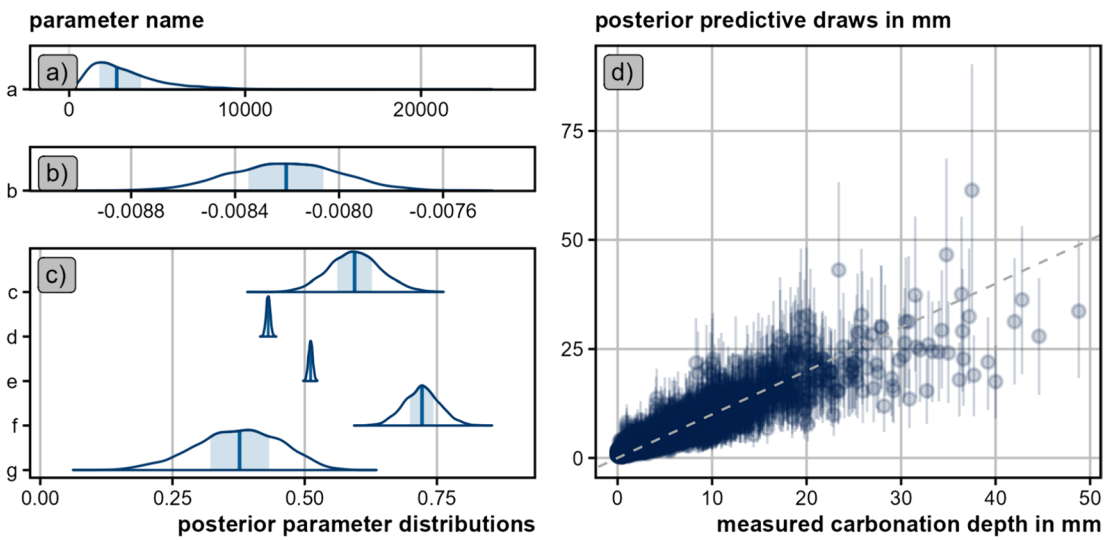

Fig. 23 Posterior distributions of the carbonation depth model parameters (**a**, **b** and **c**) and the posterior predictive check (**d**), with the MAP estimates (points) and the 90% credibility interval (error bars). The $CaO_{reactive}$ weight percentage posteriors are very similar to those from the $CaO_{reactive}$ model and are not shown here

the results are influenced by the width of the the distribution of the parameters that were used to develop the model. For example, temperature affects chemical kinetics as well as diffusion coefficients considerably (*cf.* footnote 1), but its influence on carbonation rates appears to be small. This is likely related to the fact that most of the available data relates only to temperatures around 20 °C.

8.2 Machine learning

The assessment of feature contributions to the change in carbonation depth involved employing the SHAP (SHapley Additive exPlanations) values. The SHAP summary and mean absolute values were extracted from the SHAP explainer of the model. The SHAP mean absolute value measures the global feature importance based on the magnitude of feature

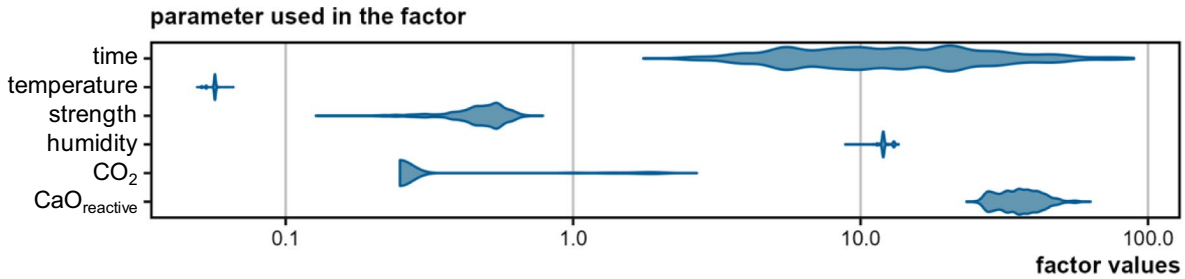

Fig. 24 Values of the different factors in the carbonation depth model product

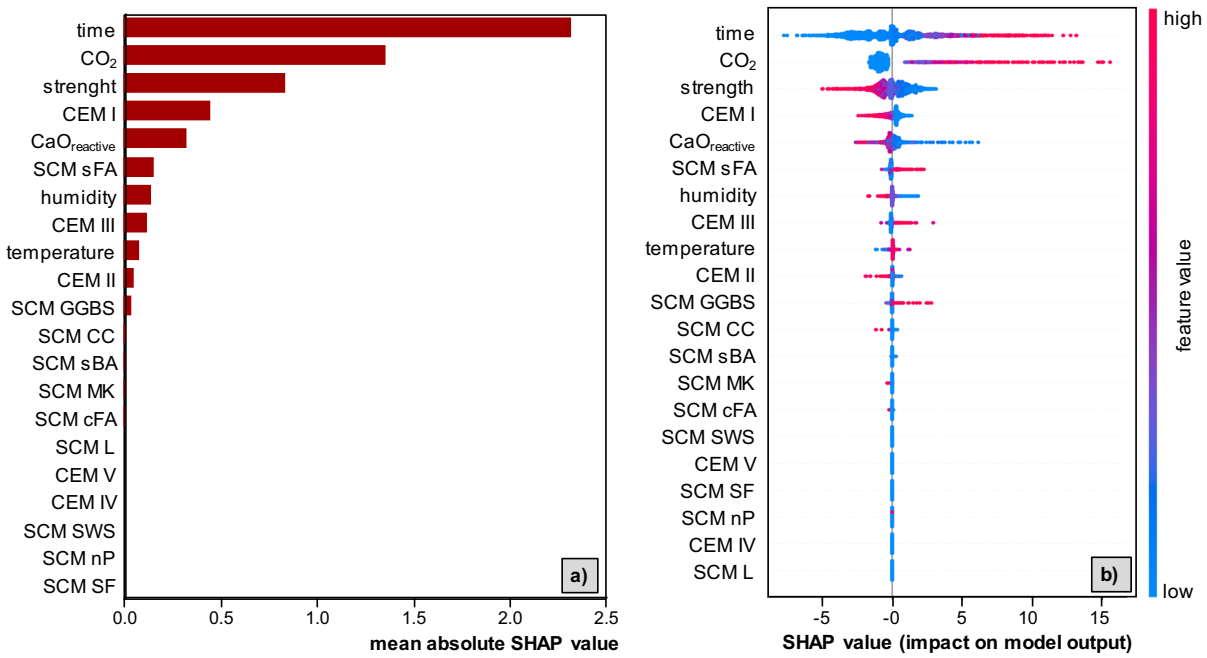

Fig. 25 (a) SHAP mean absolute (b) SHAP value

attributions, while the SHAP summary value represents the average marginal contribution of a feature value across all possible combinations of features [98].

To derive SHAP summary and mean absolute values, a machine learning model was trained. The eXtreme Gradient Boosting (XGBoost) algorithm [99] was chosen for model training and testing via a Python script. Subsequently, SHAP explainers were extracted. Additionally, a random forest model [100] underwent training, and model generalization was tested on 35% (randomly partitioned) of the dataset using both the developed random forest and XGBoost models. Evaluation of generalization performance was performed using R-squared and mean absolute error (MAE) metrics.

In Fig. 25a, the distinct importance of each feature is evident. As expected, time exhibits the highest importance, a trend also observed in Fig. 25b, which presents the SHAP summary and indicates the feature importance and the effects. The values (x-axis) indicate the average contribution of a feature to the prediction of carbonation depth in different combinations of the input features and the corresponding distribution of the values for each instance. A SHAP value to the right of the center (positive) suggests that the

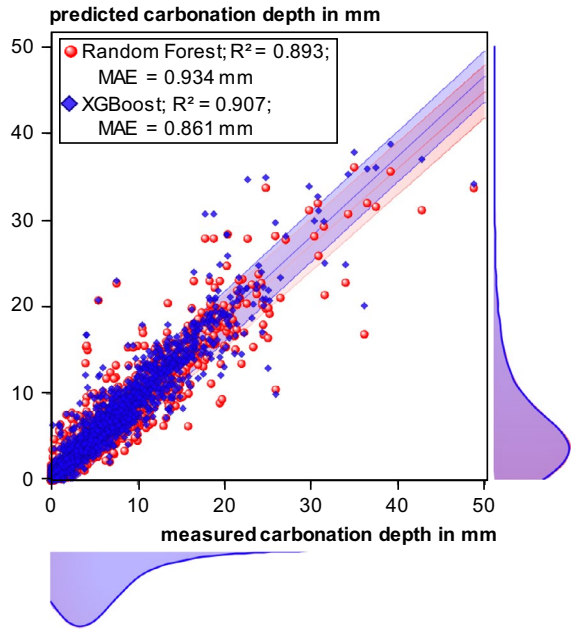

Fig. 26 Scatterplot of the measured versus predicted carbonation depth using two different machine learning approaches, for the test data subset with 0.05 prediction limits for each approach

feature pushes the model's prediction higher, while a value to the left (negative) indicates a lower prediction. The color indicates the feature's value for that particular point. The blue represent lower feature values, and red represent higher feature values. If higher values of a feature consistently lead to higher SHAP values (and thus higher predictions), this would suggest a positive correlation. If higher feature values are shown on the negative side of the plot (negative SHAP values), it implies that as the feature value increases, the effect on the model's prediction decreases. The wider distribution of CO_2 in Fig. 25b suggests less pronounced negative effects, potentially due to the constrained range of input values in the natural dataset. Moreover, strength, CEM I, humidity and $CaO_{reactive}$ contents display negative influence on the model's prediction. Other input features closer to zero in distribution may reflect their representation in the model training data. The SCMs (nP, L, SF, SWS) in the current database appear to exert minimal effects on the model's prediction. As has been briefly discussed for the temperature in Sect. 8.1, a likely reason for this is that features with a low proportion in the dataset might have a weaker influence on the model's overall prediction.

Figure 26 depicts the model generalization performance of both the random forest and XGBoost models. The random forest model trained with 21 inputs achieved an R^2 value of 0.89 and a mean absolute error of 0.934 mm, while for XGBoost, these values were 0.91 and 0.861 mm, respectively.

8.3 Discussion

Based on the above analysis, the primary factor significantly impacting carbonation depth is time. The posterior distribution of the time exponent closely aligns with square root behaviour, indicating no definitive deviation from the square root law. Even if the deviation would be real, its magnitude remains rather limited, as indicated in Fig. 27, where the MAP suggests an excess carbonation depth slightly above 10%, for a period of 100 years (exceeding the design service life of most concrete structures).

However, the exponent d associated with CO_2 concentration distinctly deviates from this behaviour (MAP value of 0.431; see also Fig. 23). This suggests

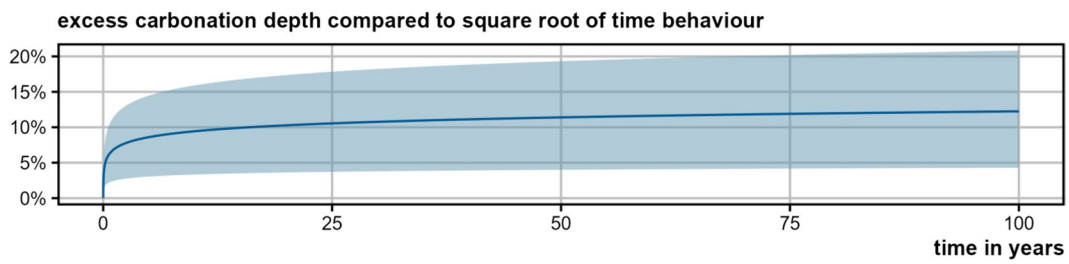

Fig. 27 Excess carbonation depth using the maximum a posteriori time exponent, compared to square root of time behaviour, in function of time. The shaded area represents the 90% credible interval

that under accelerated test conditions, carbonation might be less efficient than commonly assumed. These findings align with those in Sect. 4, wherein the prediction of natural carbonation rate from accelerated carbonation was underestimated.

Equation 8 and 9 represent the estimation of $CaO_{reactive}$ content and subsequently, the carbonation depth, utilizing the MAP parameter set. Note that the amount of SF is not included, because of rounding, as its $CaO_{reactive}$ percentage then drops to zero.

$$\begin{aligned} CaO_{reactive} = \; & 0.66 \cdot [CEMI] + 0.53 \cdot [CEMII] + 0.41 \cdot [CEMIII] + 0.35 \cdot [CEMIV] + \\ & 0.5 \cdot [CEMV] + 0.08 \cdot [sFA] + 0.06 \cdot [nP] + 0.14 \cdot [cFA] + 0.03 \cdot [CC] + \\ & 0.27 \cdot [GGBS] + 0.01 \cdot [MK] + 0.46 \cdot [SWS] + 0.01 \cdot [sBA] \end{aligned} \tag{8}$$

$$\begin{aligned} x_c = \; & 2630 \cdot 10^{-0.00821 f_c} \cdot \left(1 - \frac{RH}{100}\right)^{0.595} \\ & \cdot \left[CO_2\right]_0^{0.431} \cdot t^{0.511} \cdot [CaO]_{reactive}{}^{-0.722} \cdot 10^{-374/T} \end{aligned} \tag{9}$$

Upon comparing the results from probabilistic inference with those derived from machine learning, the mean absolute errors and R^2 values imply the potential for further enhancements in our estimations. It's worth noting that the probabilistic inference performance metrics lack a test set, suggesting a possible larger real difference, albeit there is considerable regularization through the prior distributions. The feature importance results point to the potential utility of curing time (cf. Section 5) and the water-to-binder ratio in refining our estimates. These parameters could contribute to estimating the hydration degree and porosity, thereby influencing the effective diffusivity. This information could potentially replace or complement the current reliance on compressive strength within our estimation functions. Compressive strength of concrete incorporating SCMs remains a simple and relatively reliable indicator of porosity (and therefore of its CO_2 diffusivity as suggested by the analysis in Sect. 3). Potential advantages may result from a higher degree of complexity that incorporates multiple parameters to represent the role of pore structure. The value of 0.511 for the time exponent is higher than the value resulting from the diffusion theory (0.5), but the full posterior distribution does include 0.5. Hence, we cannot conclude the square root behaviour is not valid. The data only seem to suggest that the exponent may be slightly larger than expected, and if the deviation would be real, only minor underestimation of carbonation depth could occur in practice. This seems contradictory to the usual assumption of pore structure clogging upon precipitation of carbonation products. This can be due to the particular phase assemblage of carbonated low clinker concrete or have some other origin more related with the experimental arrangements or other particularities of the analysed dataset. More research is needed to delve deeper into these aspects.

9 Conclusions

The implemented carbonation database offers the possibility to study the influence of binder composition, concrete (or mortar) mix design, curing, preconditioning, and exposure conditions on the carbonation resistance of concrete containing SCMs. The database is provided as Supplementary Information to this article and can be used for further analyses. Carbonation performance of concretes with novel binder compositions can be evaluated based on the existing data, and different test methods can be compared.

The present analysis of the database strongly supports the importance of $w/CaO_{reactive}$ as an efficient universal parameter to describe the combined effects of transport properties and buffer capacity of concrete with different types of binders. The $w/CaO_{reactive}$ ratio reflects the impact of varying binder compositions and contents on the carbonation resistance of concrete. Nevertheless, while the $w/CaO_{reactive}$ ratio captures most of the effects related to porosity on carbonation resistance, it was observed that, at the same $w/CaO_{reactive}$, concrete with higher compressive strength tends to exhibit a higher carbonation resistance. This might be related to effects of particle size distribution (of the aggregate and the binder) as well as the important effects of the curing type and period. Thus, additional parameters that are related to compressive strength, and thus also the effective diffusivity of CO_2, may further refine and improve estimates of concrete carbonation resistance.

In line with previous laboratory studies, the present analysis indicated that carbonation resistance

is not dependent on the binder content of concrete alone, i.e., it is only related to binder content via the $w/CaO_{reactive}$ ratio.

An important effect on the carbonation resistance of concretes with SCMs is exerted by the curing time before carbonation. Though present construction practices and standards leave few possibilities to exploit this potential, it appears to be worthwhile to study this effect in more detail to develop viable on-site curing regimes that yield the optimum compromise between SCM content and carbonation resistance on the one hand, and construction operation requirements on the other hand.

It has been suggested in earlier work that the relationship between the RH during carbonation and carbonation rate may be different for concretes (and mortars) based on OPC and materials based on blended cements with significant fractions of SCMs. However, since carbonation testing has so far almost always been done at a RH close to the pessimum RH for OPC concrete carbonation (60–65%), the present database did not enable the elucidation of the influence of RH on the carbonation rate of concretes with SCMs. Thus, this issue needs to be further studied in future experimental work.

Importantly, the present analysis indicated that accelerated carbonation testing (i.e., testing at CO_2 concentrations higher than 0.04%) and application of the square-root-of-time law yield predicted natural carbonation rates that tend to be lower than the corresponding measured natural carbonation rates. This effect was particularly noticeable for carbonation rates higher than ~ 0.2 mm/$\sqrt{d}$. For the materials in the present database, this value translates to $w/CaO_{reactive}$ ratios higher than ~ 1.1; i.e., the effect is especially significant for concretes with a significant SCM fraction in the binder, which is possibly the reason that it went unnoticed in several previous studies. The causes for this effect are not known in detail; thus, it is necessary to study the related phenomena in depth to be able to suggest reliable improvements of present testing standards and conversion instructions.

The predictive tool explored in the present study included many of the most relevant factors for carbonation resistance: compressive strength, RH, CO_2 concentration, $CaO_{reactive}$ content, and temperature. Unexpectedly, the probabilistic inference suggested that in the equation to predict carbonation depth, $CaO_{reactive}$ needs an exponent, which is considerably less than one. The amount of $CaO_{reactive}$ can be estimated based on the cement and SCM contents. The discrepancies between accelerated and natural carbonation tests have been quantified here, in the form of an exponent for the CO_2 concentration that is less than 0.5 (square-root behaviour), whereas only minimal deviation from progression with the square root of time was obtained. Finally, the machine learning exercise as well as the conventional analysis indicates that the curing time could be used as a parameter to further refine estimates of carbonation depth.

Acknowledgements The authors gratefully acknowledge the support by the researchers who provided additional information or unpublished data for the database: Andreas Leemann (Empa, Switzerland), Alexander Haynack (TUM, Germany), Federica Lollini (POLIMI, Italy), Christoph Müller (VDZ, Germany), Gisela Cordoba (UNICEN, Argentina), Bettina Kraft (FIB, Germany).

Funding Open Access funding enabled and organized by Projekt DEAL.

References

1. Angulo-Ramirez DE, Mejía de Gutierrez R, Valencia-Saavedra WG, de Medeiros MHF, Hoppe-Filho J (2019) Carbonation of hybrid concrete with high blast furnace slag content and its impact on structural steel corrosion. Mater Constr 69:e182
2. Atis CD (2003) Accelerated carbonation and testing of concrete made with fly ash. Constr Build Mater 17:147–152
3. Balayssac J, Detriche C, Grandet J (1995) Effects of curing upon carbonation of concrete. Constr Build Mater 9(2):91–95
4. Bonavetti VL, Cordoba G, Castellano C, Donza H, Rahhal VF, Irassar EF.: Durabilidad de hormigones con arcilla illítica calcinada y material calcáreo. X Congreso

Internacional y 24ºReunión Técnica de La Asociación Argentina de Tecnología Del Hormigón; Bonavetti, V. L, Castellano, C, Donza, H, Rahhal, V.F, Cordoba, G, & Irassar, E.F.. Hormigones de cementos compuestos con arcillas calcinadas. Revista Hormigón 60 (2022), pp 57–67
5. Brameshuber W, Schröder P.: Auswirkung der gemeinsamen Anrechnung von Silicastaub und Flugasche auf Festbetoneigenschaften. Aachen: Institute of Building Materials Research (ibac), RWTH Aachen University, 2002. Research report no. F758
6. Brameshuber W, Uebachs S.: Rationalisierungspotential bei dem Einsatz eines selbstverdichtenden Betons im Fertigteilwerk. Aachen: Institute of Building Materials Research (ibac), RWTH Aachen University, 2004. Research report no. F807
7. Brameshuber W, Pierkes R.: Anrechnung von Flugasche in Beton bei Frostbelastung gemäß der Expositionsklasse XF2 (Consideration of fly ash in concrete in case of frost attack according to exposure class XF2). Aachen: Institute of Building Materials Research (ibac), RWTH Aachen University, 2004. Research report no. F871
8. Brameshuber W, Schießl P, Uebachs S, Brandes C, Eck T.: Einfluss von Flugasche auf den Frost-Tausalz-Widerstand von Beton (Influence of fly ash on the frost resistance of concrete). Aachen: Institute of Building Materials Research (ibac), RWTH Aachen University, 2005. Research report no. F759
9. Brameshuber W, Uebachs S.: Einfluss von Flugasche auf den Frost-Tausalz-Widerstand von Beton - Ergänzende Untersuchungen für selbstverdichtende Betone mit hohem Flugaschegehalt. Aachen: Institute of Building Materials Research (ibac), RWTH Aachen University, 2008. Research report no. F827
10. Brameshuber W, Rasch S, Uebachs S, Rankers R.: Untersuchungen und Abschätzung der Leistungsfähigkeit von Hüttensanden in Bindemittel für Beton. Aachen: Institute of Building Materials Research, RWTH Aachen University, 2008. Research report no. F703
11. Brameshuber W, Vollpracht A.: Flugaschebetone gleicher Leistungsfähigkeit. Aachen: Institute of Building Materials Research (ibac), RWTH Aachen University, 2009. Research report no. F920
12. Brameshuber W, Vollpracht A, Rasch S.: Erarbeitung von Anwendungsregeln für Hüttensand als Betonzusatzstoff gemäß der harmonisierten Europäischen Stoffnorm. Aachen: Institute of Building Materials Research (ibac), RWTH Aachen University, 2009. Research report no. F7038
13. Brameshuber W, Steinhoff J.: Gemeinsame Verwendung von Flugasche und Hüttensand als Zusatzstoff im Beton. Aachen: Institute of Building Materials Research, RWTH Aachen University, 2010. Research report no. F 960/2
14. Bucher R, Diederich P, Escadeillas G, Martin C (2017) Service life of metakaolin-based concrete exposed to carbonation comparison with blended cement containing fly ash, blast furnace slag and limestone filler. Cem Concr Res 99:18–29
15. Clausen A.: Dauerhaftigkeitsbemessung und -nachweis von Tunnelinnenschalen. Aachen: Institute of Building Materials Research (ibac), faculty 3, RWTH Aachen University, 2002. Diploma thesis (unpublished)
16. Cordoba G, Sposito R, Köberl M, Zito S, Beuntner N, Tironi A, Thienel K-C, Irassar EF (2022) Chloride migration and long-term natural carbonation on concretes with calcined clays: a study of calcined clays in Argentina. Case Stud Constr Mater 17:e01190. https://doi.org/10.1016/j.cscm.2022.e01190
17. Duran-Herrera A, Mendoza-Rangel JM, De Lus Santos EU, Vasquez F, Valdez P, Bentz DP (2015) Accelerated and natural carbonation of concrete with internal curing and shrinkage/viscosity modifiers. Mater Struct 48:1207–1214
18. Etcheverry JM.: Confidential information, Ghent University - Magnel-Vandepitte Labo, Etcheverry JM Thesis, CRAHB project (2023)
19. Feldrappe V, Nobis C, Vollpracht A, Ehrenberg A, Brameshuber W.: Entwicklung von Anwendungsregeln für Hüttensandmehl als Betonzusatzstoff. Duisburg and Aachen: FEhS-Institut für Baustoff-Forschung and Institute of Building Materials Research, RWTH Aachen University, 2015. Final Report on the IGF-project 16743 N (F997)
20. Gehlen, C.: Probabilistische Lebensdauerbemessung von Stahlbetonbauwerken. Zuverlässigkeitsbetrachtungen zur wirksamen Vermeidung von Bewehrungskorrosion. Berlin Beuth, Schriftenreihe des Deutschen Ausschusses für Stahlbeton, Nr. 510 (2000), ISBN 978–3–410–65710–1
21. Greve-Dierfeld S.: Bemessungsregeln zur Sicherstellung der Dauerhaftigkeit von XC exponierten Stahlbetonbauteilen. Dissertation TU München 2015
22. Gruyaert E, Van den Heede P, De Belie N (2013) Carbonation of slag concrete: effect of the cement replacement level and curing on the carbonation coefficient – effect of carbonation on the pore structure. Cement Concr Compos 35:39–48
23. Holthuizen PE, Çopuroğlu O, Polder RB (2018) Chloride ingress of carbonated blast furnace slag cement mortars High Tech Concrete – Where Technology and Engineering Meet. Springer, Cham, pp 73–82
24. Hunkeler F, Lammar L.: Anforderungen an den Karbonatisierungswiderstand von Betonen (Requirements on the carbonation resistance of concrete mixes). Forschungsauftrag AGB 2008/012 auf Antrag der Arbeitsgruppe Brückenforschung (AGB), Nov. 2012
25. ibac: confidential material testing reports. Institute of Building Materials Research (ibac), RWTH Aachen University
26. Iloro F.H.: Efectos del CO2 ambiental sobre la carbonatación de hormigones elaborados con distintos cementos, PhD Thesis, Universidad Nacional del Sur, Bahia Blanca, Argentina (2022), p 284 https://lemit.gov.ar/documentos/tesis/tesis_doctor_f_h_iloro.rar
27. Kamali-Bernard S, Muy Y, Piolet E, Brossault J.Y.: Carbonatation naturelle et carbonatation accélérée selon le mode opératoire européen d'un lot de 4 bétons. Rapport PERF/R/097 - LGCGM - Projet National PerfDuB (2021) and Fonollosa, P, Fabrication de 11 bétons avec granulats G2, Rapport PERF/R/112 - Bouygues TP - Projet National PerfDuB (2021)

28. Kraft B, Achenbach R, Ludwig H-M, Raupach M (2022) Hydration and Carbonation of alternative Binders. Corros Mater Degrad 3:19–52. https://doi.org/10.3390/cmd3010003
29. Achenbach R, Kraft B, Ludwig H-M, Raupach M (2021) Dauerhaftigkeit von alternativen Bindemitteln (Durability of alternative Binders). Beton- und Stahlbeton. https://doi.org/10.1002/best.202100056
30. Kraft B, Müller M, Achenbach R, Ludwig H-M, Raupach M (2023) Influence of CO_2 concentration during accelerated carbonation tests with alternative binders. Nano World J. https://doi.org/10.17756/nwj.2023-s2-034
31. Leemann A, Nygaard P, Kaufmann J, Loser R (2015) Relation between carbonation resistance, mix design and exposure of mortar and concrete. Cement Concr Compos 62:33–43
32. Leemann A, Moro F (2017) Carbonation of concrete: The role of CO_2 concentration, relative humidity and CO_2 buffer capacity. Mater Struct 50:30
33. Leeman A, Pahlke H, Loser R, Winnefeld F (2018) Carbonation resistance of mortar produced with alternative cements. Mater Struct 51:114
34. Lee J, Lee T, Choi H, Lee DE (2020) Assessment of optimum CaO content range for high volume FA based concrete considering durability properties. Appl Sci 10:6944
35. Lollini F, Redaelli E (2021) Carbonation of blended cement concretes after 12 years of natural exposure. Constr Build Mater 276:122122
36. Martins IM, Goncalves A, Marques JC.: Durability and Strength Properties of Concrete Containing Coal Bottom Ash. Bagneux: RILEM, 2010. Proceedings of the International RILEM Conference on Materials Science (MatSci), Vol. III: Additions Improving Properties of Concrete (AdIPoC), Aachen, September 6–8, 2010, (Brameshuber, W. (Ed.)), p. 275–283 - *additional information provided by the authors.*
37. Msinjili NS, Vogler N, Sturm P, Neubert M, Schröder H-J, Kühne H-C, Hünger K-J, Gluth GJG (2021) Calcined brick clays and mixed clays as supplementary cementitious materials: effects on the performance of blended cement mortars. Constr Build Mater 266:120990. https://doi.org/10.1016/j.conbuildmat.2020.120990
38. Müller C, FIZ; FEhS.: Dauerhaftigkeit von Betonen unter Verwendung von Zementen mit mehreren Hauptbestandteilen (Teil 1: Zemente mit bis zu 35 M.-% Kalkstein in Kombination mit Hüttensand). Düsseldorf and Duisburg: Forschungsinstitut der Zementindustrie und Forschungsgemeinschaft (FIZ) Eisenhüttenschlacken e. V. (FEhS), 2004. Final report of the IGF-project 13332 N
39. Müller C, Lang E.: Dauerhaftigkeit von Beton mit Portlandkalkstein- und Portlandkompositzementen CEM II-M (S-LL) (Durability of concrete made with Portland limestone and Portland composite cements CEM II-M (S-LL)). Betontechnische Berichte 2004–2006; Düsseldorf: Verein Deutscher Zementwerke, Verlag Bau+Technik (2007), pp 29–52
40. Müller C, Severins K (2012) VDZ gGmbH: Schlussbericht zum Forschungsvorhaben „NanoCarbo“, Förderkennzeichen 03X0070, Verbesserung der Dauerhaftigkeit von Betonen mit hüttensandhaltigen Zementen durch Verringerung der Carbonatisierungsempfindlichkeit. Forschungsinstitut der Zementindustrie, Betontechnik, Düsseldorf
41. Newlands M.: Development of a simulated natural carbonation test of selected CEM II concretes. Phd thesis, University Dundee 2001.
42. Pico-Cortés C, Zega C, Villagrán-Zaccardi Y.: Desempeño en ambiente natural de hormigones diseñados para resistir carbonatación, XVI Congreso Latinoamericano de Patología de la Construcción y XVIII de Control de Calidad en la Construcción, 19–21 October 2021, Iguacu, Brazil, pp 804–817. https://doi.org/10.4322/conpat2021.460
43. Rathnarajan S, Dhanya BS, Pillai RG, Gettu R, Santhanam M (2022) Carbonation model for concretes with fly ash, slag, and limestone calcined clay - using accelerated and five - year natural exposure data. Cement Concr Compos 126:104329
44. Rumman R, Kamal MR, Manzur T, Noor MA (2022) Optimum proportion of fly ash or slag for resisting concrete deterioration due to carbonation and chloride ingress. Structures 41:287–305
45. Scholz E, Wierig H.-J.: Untersuchungen über den Einfluß von Flugaschezusätzen auf das Carbonatisierungsverhalten von Beton. I. Ergänzung 1988. Hannover: Institut für Baustoffkunde und Materialprüfung, 1985; 1988. - (Forschungsbericht)
46. Schieß, P, Härdtl R.: Untersuchungen an Mörteln und Betonen mit Steinkohlenflugasche für eine erweiterte Anrechenbarkeit der Steinkohlenflugasche, parts I, II und documentary volume. Aachen: Institute of Building Materials Research (ibac), RWTH Aachen University, 1992. Research report no. F236 and F323
47. Schießl P, Wiens U, Breit W.: Reduzierung des Alkalitätsdepots durch Puzzolane (Reduction of the reserve alkalinity by pozzolangs). Aachen: Institute of Building Materials Research (ibac), RWTH Aachen University, 1994. Research report no. F397
48. Schießl P, Müller C.: Baustoffkreislauf im Massivbau (BiM) - Bewertung der bei der Aufbereitung von Bauschutt anfallenden Recyclingzuschläge hinsichtlich der Eignung als Betonzuschlag. BiM-Project-no. D/03. Aachen: Institute of Building Materials Research (ibac), 1997. Research report no. F 1550/1
49. Troconis de Rincón O, Montenegro JC, Vera R, Carvajal AM, Mejía de Gutierrez R, Del Vasto S, Saborio E, Torres-Acosta A, Pérez-Quiroz J, Martínez-Madrid M, Martinez-Molina W, Alonso-Guzmán E, CastroBorges P, Moreno EI, Almeraya-Calderón F, Gaona-Tiburcio C, Pérez-López T, Salta M, de Melo AP, Martínez I, Rebolledo N, Rodríguez G, Pedrón M, Millano V, Sánchez M, de Partidas E.: Concrete Carbonation in Ibero-American Countries - DURACON Project: Six-Year Evaluation, Corrosion, Vol. 71 (2015), No. 4, 546–555
50. TUM: unpublished data from the Technical University of Munich, 2017
51. Vanoutrive H, Van den Heede P, Alderete N, Andrade C, Bansal T, Camões A, Cizer Ö, De Belie N, Ducman V, Etxeberria M, Frederickx L, Grengg C, Ignjatović I, Ling T-C, Liu Z, Garcia-Lodeiro I, Lothenbach B,

Medina Martinez C, Sanchez-Montero J, Olonade K, Palomo A, Phung QT, Rebolledo N, Sakoparnig M, Sideris K, Thiel C, Visalakshi T, Vollpracht A, von Greve-Dierfeld S, Wei J, Wu B, Zając M, Zhao Z, Gruyaert E (2022) Report of RILEM TC 281-CCC: outcomes of a round robin on the resistance to accelerated carbonation of Portland, Portland-fly ash and blast-furnace blended cements. Mater Struct 55:99. https://doi.org/10.1617/s11527-022-01927-7

52. Vanoutrive, H, Alderete, N, De Belie, N, Etxeberria, M, Grengg, C, Ignjatović, I, Ling, T.-C, Liu, Z, Garcia-Lodeiro, I, Medina Martinez, C, Sanchez-Montero, J, Palomo, A, Rebolledo, N, Sakoparnig, M, Sideris, K, Thiel, C, Van den Heede, P, Vollpracht, A, von Greve-Dierfeld, S, Wei, J, Zając, M, Gruyaert, E.: Report of RILEM TC 281-CCC: Outcomes of a round robin on the resistance to natural carbonation of Portland, Portland fly ash and blast-furnace blended cements and its relation to accelerated carbonation. *Submitted to Materials and Structures (2024)*
53. Younsi A, Turcry P, Ait-Mokhtar A (2022) Quantification of CO_2 uptake of concretes with mineral additions after 10-year natural carbonation. J Clean Prod 349:131362. https://doi.org/10.1016/j.jclepro.2022.131362
54. Zega, C.J, Etcheverry, J.M, Villagrán Zaccardi, Y.A.: Natural carbonation of multiply recycled aggregate concrete, International Workshop CO2 Storage in Concrete, 24–25 June 2019, Marne la Vallée, France, pp 117–123
55. von Greve-Dierfeld S, Lothenbach B, Vollpracht A, Wu B, Huet B, Andrade C, Medina C, Thiel C, Gruyaert E, Vanoutrive H, Saéz del Bosque IF, Ignjatovic I, Elsen J, Provis J.L, Scrivener K, Thienel K.-C, Sideris K, Zajac M, Alderete N, Cizer Ö, Van den Heede P, Hooton D, Kamali-Bernard S, Bernal S.A, Zhao Z, Shi Z, De Belie N.: Understanding the carbonation of concrete with supplementary cementitious materials: a critical review by RILEM TC 281-CCC. Materials and Structures 53 (2020), p 136 (34 pages)
56. Vollpracht A, Thiel C, Zhao Z, Villagran Zaccardi YA, Cordoba GP, Gluth GJG, Vanoutrive H, Gruyaert E, Kanellopolous A, Mi R, Belie de N.: Carbonation of Concrete with SCMs: A Data Analysis by RILEM TC 281-CCC. Proceedings of the 16th International Congress on the Chemistry of Cement, Volume III, Bangkok, Thailand, September, 18–22, 2023, pp 360–363
57. Ipavec A, Gabrovšek R, Vuk T, Kaučič V, Maček J, Meden A (2011) Carboaluminate phases formation during the hydration of calcite-containing Portland cement. J Am Ceramic Soc 94:1238–1242. https://doi.org/10.1111/j.1551-2916.2010.04201.x
58. De Weerdt K, Ben Haha M, Le Saout G, Kjellsen KO, Justnes H, Lothenbach B (2011) Hydration mechanisms of ternary Portland cements containing limestone powder and fly ash. Cem Concr Res 41:279–291. https://doi.org/10.1016/j.cemconres.2010.11.014
59. Glasser FP, Matschei T.: Interactions between Portland cement and carbon dioxide. Proceedings of the 12th International Congress on the Chemistry of Cement, Montréal, Canada, 2007. paper no. TH3–13.4
60. Taylor HFW (1997) Cement chemistry, 2nd edn. Thomas Telford, London
61. Steiner S, Lothenbach B, Proske T, Borgschulte A, Winnefeld F (2020) Effect of relative humidity on the carbonation rate of portlandite, calcium silicate hydrates and ettringite. Cem Concr Res 135:106116. https://doi.org/10.1016/j.cemconres.2020.106116
62. Buenfeld NR, Okundi E (1998) Effect of cement content on transport in concrete. Mag Concr Res 50:339–351. https://doi.org/10.1680/macr.1998.50.4.339
63. Wassermann R, Katz A, Bentur A (2009) Minimum cement content requirements: a must or a myth? Mater Struct 42:973–982. https://doi.org/10.1617/s11527-008-9436-0
64. Page CL, Treadaway KWJ (1982) Aspects of the electrochemistry of steel in concrete. Nature 297:109–115. https://doi.org/10.1038/297109a0
65. Papadakis VG, Vayenas CG, Fardis MN (1991) Fundamental modeling and experimental investigation of concrete carbonation. ACI Mater J 88:363–373
66. Sisomphon K, Franke L (2007) Carbonation rates of concretes containing high volume of pozzolanic materials. Cem Concr Res 37:1647–1653. https://doi.org/10.1016/j.cemconres.2007.08.014
67. Van den Heede P, De Schepper M, De Belie N (2019) Accelerated and natural carbonation of concrete with high volumes of fly ash: chemical, mineralogical and microstructural effects. Royal Society Open Science Jounal 6:181665. https://doi.org/10.1098/rsos.181665
68. Van den Heede P, De Belie N (2021) Effects of accelerated carbonation testing and by-product allocation on the CO2-sequenstration-to-emission ratios of fly ash-based binder systems. Appl Sci 11:2781. https://doi.org/10.3390/app11062781
69. Gluth GJG, Ke X, Vollpracht A, Weiler L, Bernal SA, Cyr M, Dombrowski-Daube K, Geddes DA, Grengg C, Le Galliard C, Nedeljkovic M, Provis JL, Valentini L, Walkley B (2022) Carbonation rate of alkali-activated concretes and high-volume SCM concretes: a literature data analysis by RILEM TC 281-CCC. Mater Struct 55:225. https://doi.org/10.1617/s11527-022-02041-4
70. Chanut S, Cussigh F, Fabbris F, Linger L, Mai-Nhu J, Moro F, Pernin T, Pham G, Potier J.-M, Rougeau P, Rozière E, Toutlemonde F, Turcry P.: Base de données et son exploitation. In: Approche performantielle de la durabilité des ouvrages en béton: de la qualification en laboratoire au suivi d'exécution - Projet National PerfDuB. Éditions Eyrolles, (2023)
71. Hunkeler F, Lammar L.: Anforderungen an den Karbonatisierungswiderstand von Betonen. Forschungsbericht AGB 2008/012. Eidgenössisches Departement UVEK/Bundesamt für Strassen, (2012)
72. Saillio M.: Interactions physiques et chimiques ions-matrice dans les bétons sains et carbonatés. Influence sur le transport ionique. Thèse (2012), Université Paris Est
73. Bertin M.: L'impact du séchage au jeune âge sur la carbonatation des matériaux cimentaires avec additions minerals. Thèse (2018), Université de Paris Est-Marne La Vallée

74. Rozière E.: Etude de la durabilité des bétons par und approche performantielle. Thèse (2007), Université de Nantes
75. Buenfeld NR, Yang R.: On-site curing of concrete – microstructure and durability. Construction Industry Research and Information Association, CIRIA 2001, ISBN 0 86017 5308
76. Thiel C, Kratzer J, Grimm B, Kränkel T, Gehlen C (2022) Effect of Internal Moisture and Outer Relative Humidity on Concrete Carbonation. CivilEng 3:1039–1052. https://doi.org/10.3390/civileng3040058
77. Forsdyke JC; Lees JM.: Carbonation depth measurement of concretes exposed to different curing and preconditionning conditions, using image-processing tools. Proc. of the 2nd fib Symposium on Concrete and Concrete Structures, Nov 18th -19th, 2021, Sapienza University, Rome, Italy
78. Soja W, Georget F, Maraghechi H, Scrivener K (2020) Evolution of microstructural changes in cement paste during environmental drying. Cem Concr Res 134:106093. https://doi.org/10.1016/j.cemconres.2020.106093
79. Thiel C.: Einfluss von CO_2-Druck und Feuchtegehalt auf das Porengefüge von zementgebundenen Materialien während der Carbonatisierung. Dissertation (2023), Technical University of Munich
80. Wierig H-J (1986) Die Carbonatisierung des Betons. Naturstein Ind 22(5):26–35
81. Cussler EL (2009) Diffusion: mass transfer in fluid systems. Cambridge University Press, Cambridge
82. Bird RB, Stewart WE, Lightfoot EN (2007) Transport phenomena, 2nd edn. Wiley, New York
83. Parrott LJ (1991) Factors influencing relative humidity in concrete. Mag Concr Res 43:45–52. https://doi.org/10.1680/macr.1991.43.154.45
84. Nilsson L-O (2023) Predicting moisture in field concrete - decisive parameters. Cement 11:100052. https://doi.org/10.1016/j.cement.2022.100052
85. Andrade C, Sarría J, Alonso C (1999) Relative humidity in the interior of concrete exposed to natural and artificial weathering. Cement Concr Res 29:1249–1259. https://doi.org/10.1016/S0008-8846(99)00123-4
86. Vu QH, Pham G, Chonier A, Brouard E, Rathnarajan S, Pillai R, Sarnot A (2019) Impact of different climates on the resistance of concrete to natural carbonation. Constr Build Mater 216:450–467. https://doi.org/10.1016/j.conbuildmat.2019.04.263
87. R Core Team: R A Language and Environment for Statistical Computing. Vienna, Austria: R Foundation for Statistical Computing (2023). https://www.R-project.org/
88. Wickham H, Averick M, Bryan J, Chang W, D'Agostino McGowan L, Garrett Grolemund R-F et al (2019) Welcome to the tidyverse. J Open Sour Softw 4(43):1686. https://doi.org/10.21105/joss.01686
89. Wickham H (2014) Tidy Data. J Stat Softw 59(10):1–23. https://doi.org/10.18637/jss.v059.i10
90. Stan Development Team: Stan Modeling Language Users Guide and Reference Manual, 2.33 (2023). https://mc-stan.org
91. Gabry J, Češnovar R, Johnson A.: Cmdstanr: R Interface to 'CmdStan' (2022)
92. Papadakis VG, Vayenas CG, Fardis MN (1989) A reaction engineering approach to the problem of concrete carbonation. AIChE J 35(10):1639–1650
93. Wang X-Y, Lee H-S (2009) A model for predicting the carbonation depth of concrete containing low-calcium fly ash. Constr Build Mater 23(2):725–733
94. You X, Hu X, He P, Liu J, Shi C (2022) A review on the modelling of carbonation of hardened and fresh cement-based materials. Cement Concr Compos 125:104315
95. Papadakis VG, Vayenas CG, Fardis MN (1991) Physical and Chemical Characteristics Affecting the Durability of Concrete. ACI Mater J 88(2):186–196
96. Li G, Yuan Y, Du J, Ji Y (2013) Determination of the apparent activation energy of concrete carbonation. J Wuhan Univ Technol-Mater Sci Ed 28:944–949
97. Muntean A, Meier SA, Peter MA, Böhm M, Kropp J.: A Note on Limitations of the Use of Accelerated Concrete-Carbonation Tests for Service-Life Predictions." Berichte Aus Der Technomathematik; Vol. 0504 (2005); Universität Bremen.
98. Molnar, C.: Interpretable Machine Learning A Guide for Making Black Box Models Explainable. (2024). https://christophm.github.io/interpretable-ml-book/
99. Tianqi C, Guestrin C, Boost XG.: A Scalable Tree Boosting System. Proceedings of the 22nd ACM SIGKDD International Conference on Knowledge Discovery and Data Mining (KDD '16). Association for Computing Machinery, New York, USA (2016), p. 785–794. https://doi.org/10.1145/2939672.2939785
100. Breiman L (2001) Random forests. Mach Learn 45:5–32